

# $(g - 2)_{e,\mu}$ anomalies and decays $h, Z \rightarrow e_b e_a$ in 3-3-1 models with inverse seesaw neutrinos

T.T. Hong,<sup>1,2,\*</sup> L.T.T. Phuong,<sup>1,2,†</sup> T.Phong  
Nguyen,<sup>3,‡</sup> N.H.T. Nha,<sup>4,5,§</sup> and L. T. Hue<sup>e4,5,\*\*</sup>

<sup>1</sup>*An Giang University, Long Xuyen City 880000, Vietnam*

<sup>2</sup>*Vietnam National University, Ho Chi Minh City 700000, Vietnam*

<sup>3</sup>*Department of Physics, Can Tho University,  
3/2 Street, Ninh Kieu, Can Tho City 94000, Vietnam*

<sup>4</sup>*Subatomic Physics Research Group,  
Science and Technology Advanced Institute,  
Van Lang University, Ho Chi Minh City, Vietnam*

<sup>5</sup>*Faculty of Applied Technology, School of Technology,  
Van Lang University, Ho Chi Minh City, Vietnam*

## Abstract

The lepton flavor violating (LFV) decays  $h, Z \rightarrow e_b e_a$ , and  $e_b \rightarrow e_a \gamma$  are discussed in a class of general 3-3-1 models adding heavy neutral leptons and singly charged Higgs bosons to accommodate experimental data of neutrino oscillation and  $(g - 2)_{e_a}$  anomalies of charged leptons through the inverse seesaw mechanism. We show that the models with the minimal number of inverse seesaw neutrinos cannot reach the  $1\sigma$  range of  $(g - 2)_\mu$  data due to the experimental upper bounds on decay rates of  $(\tau \rightarrow \mu \gamma)$  and  $(\mu \rightarrow e \gamma)$ . Features of LFV decays are presented in detail, focusing on the regions of parameter space satisfying the  $1\sigma$  ranges of  $(g - 2)_{e,\mu}$  data.

---

<sup>e</sup> Corresponding author

\* tthong@agu.edu.vn

† lttphuong@agu.edu.vn

‡ thanhphong@ctu.edu.vn

§ nguyenuathanhnhha@vlu.edu.vn

\*\* lethohue@vlu.edu.vn

## I. INTRODUCTION

Based on the original works [1–4], a general class of 3-3-1 models constructed from the gauge group  $SU(3)_C \otimes SU(3)_L \otimes U(1)_X$  was introduced [5–7], in which new exotic leptons carrying arbitrary electric charges as functions of a parameter  $\beta$  ( $331\beta$ ). Various phenomenologies of this model class were discussed [7–14], indicating a large lower bound of  $\mathcal{O}(10)$  TeV for  $SU(3)_L$  scale and heavy singly charged Higgs boson masses. Moreover, this  $331\beta$  model consisting of six new inverse seesaw (ISS) neutrinos, named the  $331\beta$ ISS model, and a singly charged Higgs boson can explain successfully both the  $(g - 2)_{e,\mu}$  data and the neutrino oscillation data. In this work, we continue discussing properties of the lepton flavor violating (LFV) decays of the standard-model-like (SM-like) and  $Z$  bosons, denoted as  $LFVh$  and  $LFVZ$ , respectively. The correlations with LFV decays of charged leptons (cLFV)  $e_b \rightarrow e_a\gamma$  will be investigated also. Other extensions of 3-3-1 models with new vectorlike fermions, leptoquarks, or/and scalars [14–18] can accommodate the  $(g - 2)_\mu$  anomalies and cLFV experimental constraints, but the correlations between LFV decays of  $h$  and  $Z$  bosons and updated  $(g - 2)_{e_a}$  data have not been mentioned.

Normally, the  $331$ ISS models discussed previously consist of six ISS neutrinos, although the minimal number can be 4, well known as minimal ISS (mISS) models, which reduce a significant number of independent couplings, therefore is predictive for the correlations between  $(g - 2)_{e,\mu}$  and LFV decays. The mISS models were shown to accommodate the neutrino oscillation data and the observed baryon asymmetry from the presence of the minimal number of new neutral heavy leptons with masses at TeV scale [19–22]. The LFV source will generate one-loop contributions to cLFV decays such as  $e_b \rightarrow e_a\gamma$ ,  $LFVh$ ,  $LFVZ$ , etc . . . . In this work, we will introduce LFV sources as well as LFV one-loop contributions in the general  $331\beta$ ISS( $K, K$ ) framework having  $2K$  heavy ISS neutrinos. After that, we will focus on two simple frameworks of  $331\beta$ mISS and the  $331\beta$ ISS with  $(3, 3)$  ISS neutrinos, in which the possibility to accommodate both the  $(g - 2)_{e,\mu}$  data and LFV decay rates will be investigated numerically. The ISS mechanisms with  $2K > 6$  [153] such as the double ISS one may be investigated in our future work.

Experimental data for  $(g - 2)_{e,\mu}$  anomalies have been updated from Ref. [23] showing a  $5.1\sigma$  standard deviation from the SM prediction [24–51] that  $\Delta a_\mu^{\text{NP}} \equiv a_\mu^{\text{exp}} - a_\mu^{\text{SM}} = (2.49 \pm 0.48) \times 10^{-9}$  [52]. The experimental  $a_e$  data were reported from different groups [53–

56], leading to the two inconsistent deviations between experiments and the SM prediction [57–62]. In this work, we chose the value  $\Delta a_e^{\text{NP}} = (3.4 \pm 1.6) \times 10^{-13}$ , using the latest experimental data for  $a_e^{\text{exp}}$  [55]. Although another  $a_e^{\text{SM}}$  result was derived [54], leading to a  $3.9\sigma$  deviation that  $\Delta a_e^{\text{NP}} = (-10.2 \pm 2.6) \times 10^{-13}$ , which has the same magnitude order as the first result. Therefore, we choose one of them for illustration.

The cLFV rates are constrained from recent (future) experiments as follows [63–66] ([67, 68]):  $\text{Br}(\mu \rightarrow e\gamma) < 3.1 \times 10^{-13}$  ( $6 \times 10^{-14}$ ),  $\text{Br}(\tau \rightarrow e\gamma) < 3.3 \times 10^{-8}$  ( $9 \times 10^{-9}$ ), and  $\text{Br}(\tau \rightarrow \mu\gamma) < 4.2 \times 10^{-8}$  ( $6.9 \times 10^{-9}$ ). The latest experimental constraints for LFVh decay rates are  $\text{Br}(h \rightarrow \tau\mu) < 1.5 \times 10^{-3}$ ,  $\text{Br}(h \rightarrow \tau e) < 2 \times 10^{-3}$ , and  $\text{Br}(h \rightarrow \mu e) < 4.4 \times 10^{-5}$  [69–72]. The future sensitivities at the high-luminosity Large Hadron Collider (HL-LHC) and  $e^+e^-$  colliders may be orders of  $\mathcal{O}(10^{-4})$ ,  $\mathcal{O}(10^{-4})$ , and  $\mathcal{O}(10^{-5})$  for the three above LFVh decays, respectively [73–76].

The latest experimental constraints for LFVZ decay rates are  $\text{Br}(Z \rightarrow \tau^\pm\mu^\mp) < 6.5 \times 10^{-6}$ ,  $\text{Br}(Z \rightarrow \tau^\pm e^\mp) < 5.0 \times 10^{-6}$ , and  $\text{Br}(Z \rightarrow \mu^\pm e^\mp) < 2.62 \times 10^{-7}$  [77, 78]. The future sensitivities will be  $10^{-6}$ ,  $10^{-6}$ , and  $7 \times 10^{-8}$  at HL-LHC and  $10^{-9}$ ,  $10^{-9}$ , and  $10^{-10}$  at FCC-ee [79, 80], respectively. These LFVZ decays were shown theoretically as promoting signals of new physics that are visible for incoming experimental searches [81–91]. They will be discussed in the  $331\beta\text{ISS}$  model, concentrating on the allowed regions of parameters successfully explaining the  $(g - 2)_{e,\mu}$  data.

Our paper is organized as follows. In Sec. II we briefly review the  $331\beta\text{ISS}(K, K)$  model, determining all physical states, masses and mixing parameters of all leptons. In Sec. III, we compute all relevant couplings, Feynman rules relating to one-loop LFV contributions, and analytic formulas for  $(g - 2)_{e,\mu}$  anomalies and LFV decay rates. Interestingly, we introduce a general analytic expression dominant one-loop contributions to  $(g - 2)_{e,\mu}$  and LFV amplitudes, arising from the well-known "chiral enhancement" ones. From this, we will indicate a strict relation between  $\Delta a_\mu$  and  $\text{Br}(\tau \rightarrow \mu\gamma)$  in the  $331\beta\text{mISS}$  framework. The numerical illustrations for various relations among LFV decay rates and  $\Delta a_{e,\mu}$  and important parameters of the two  $331\beta\text{mISS}$  and  $331\beta\text{ISS}$  are depicted in Sec. IV. Important features discussed in our work are summarized in Sec. V. Finally, there are four Appendices showing precisely the Higgs sector, master functions relating to formulas of  $\Delta a_{e_a}$ , and general one-loop contributions to LFVZ and LFVh decay amplitudes. These formulas are constructed in the general case of  $2K$  ISS neutrinos, being very useful for further studying the  $331\beta$

models consisting of various ISS neutrino kinds mentioned in Ref. [153].

## II. REVIEW THE 3-3-1 MODEL WITH ISS NEUTRINOS

Here, we summarize the most important content of the  $331\beta\text{ISS}(K, K)$  model relating to our work. The lepton sector and charged lepton masses and mixing parameters were shown in detail in Ref. [92], where left-handed (LH) leptons are assigned to antitriplets and right-handed (RH) leptons are singlets

$$\begin{aligned} L'_{aL} &= \left( e'_a \quad -\nu'_a \quad E'_a \right)_L^T \sim \left( 3^*, -\frac{1}{2} + \frac{\beta}{2\sqrt{3}} \right), \quad a = 1, 2, 3, \\ e'_{aR} &\sim (1, -1), \quad \nu_{IR}, X_{IR} \sim (1, 0), \quad E'_{aR} \sim \left( 1, -\frac{1}{2} + \frac{\sqrt{3}\beta}{2} \right), \end{aligned} \quad (1)$$

where we just pay attention to the  $SU(3)_L \otimes U(1)_X$  group. In general, we consider that the model includes  $2K$  RH neutrinos as  $SU(3)_L$  singlets, namely,  $\nu_{IR}$  and  $X_{IR}$  with  $I = \overline{1, K}$ . The prime denotes flavor states which are generally different from the mass eigenstates.

The quark sector is ignored here; see detail in Refs. [7–9] for example. The class of models constructed using  $SU(3)_L$  antitriplet LH fermions defined in Eq. (1) is equivalent to the one using triplets through a transformation keeping physical results unchanged [92, 93].

The covariant derivative defined by the electroweak (EW) gauge group  $SU(3)_L \otimes U(1)_X$  is  $D_\mu \equiv \partial_\mu - igT^a W_\mu^a - ig_X X T^9 X_\mu$ , where  $T^9 = 1/\sqrt{6}$ ,  $g$ , and  $g_X$  are gauge couplings of the two groups  $SU(3)_L$  and  $U(1)_X$ , respectively. In general, the model  $331\beta$  model predicts three charged gauge bosons:  $W_\mu^\pm = \frac{1}{\sqrt{2}} (W_\mu^1 \mp iW_\mu^2)$ ,  $Y_\mu^{\pm A} = \frac{1}{\sqrt{2}} (W_\mu^4 \mp iW_\mu^5)$ , and  $V_\mu^{\pm B} = \frac{1}{\sqrt{2}} (W_\mu^6 \mp iW_\mu^7)$ . The new electric charges of the gauge and Higgs bosons, and charged leptons are  $A = \frac{1}{2} + \frac{\sqrt{3}\beta}{2}$  and  $B = -\frac{1}{2} + \frac{\sqrt{3}\beta}{2}$ . Three scalar triplets needed for generating masses are

$$\begin{aligned} \chi &= \left( \chi_A \quad \chi_B \quad \chi^0 \right)^T \sim \left( 3, \frac{\beta}{\sqrt{3}} \right), \quad \rho = \left( \rho^+ \quad \rho^0 \quad \rho^{-B} \right)^T \sim \left( 3, \frac{1}{2} - \frac{\beta}{2\sqrt{3}} \right), \\ \eta &= \left( \eta^0 \quad \eta^- \quad \eta^{-A} \right)^T \sim \left( 3, -\frac{1}{2} - \frac{\beta}{2\sqrt{3}} \right), \end{aligned} \quad (2)$$

and a new singly charged Higgs boson  $h^+ \sim (1, 1, 1)$ , needed for generating large one-loop contributions to  $(g-2)_{e_a}$  anomalies. Nonzero vacuum expectation values (VEVs) of neutral Higgs components are

$$\langle \chi^0 \rangle = \frac{v_3}{\sqrt{2}}, \quad \langle \rho^0 \rangle = \frac{v_2}{\sqrt{2}}, \quad \langle \eta^0 \rangle = \frac{v_1}{\sqrt{2}}. \quad (3)$$

In addition, two Higgs triplets can play roles as those in the well-known two-Higgs-doublet models (2HDM) in generating masses for SM fermions in the 3-3-1 models [9]. Therefore, we use a notation appearing in the 2HDM that  $t_\beta \equiv \frac{v_2}{v_1}$ , so that  $s_\beta^2 + c_\beta^2 = 1$ , following the notations that  $s_x \equiv \sin \theta_x$ ,  $c_x \equiv \cos \theta_x$ , and  $t_x \equiv \tan \theta_x$ , which will be used from now on.

The symmetry breaking patterns for the EW of the 331 $\beta$  model are :  $SU(3)_L \otimes U(1)_X \xrightarrow{v_3} SU(2)_L \otimes U(1)_Y \xrightarrow{v_1, v_2} U(1)_Q$ , leading to the condition that  $v_3 \gg v_1, v_2$ . The first breaking step result in four massless gauge bosons identified with the SM ones. Consequently, the  $SU(3)_L$  gauge couplings are determined as

$$t_X \equiv \frac{g_X}{g} = \frac{\sqrt{6}s_W}{\sqrt{1 - (1 + \beta^2)s_W^2}}, \quad g = g_2, \quad (4)$$

where the weak mixing angle is defined as  $t_W = \tan \theta_W = g_1/g_2$  and  $g_{1,2}$  are the  $U(1)_Y$  and  $SU(2)_L$  gauge couplings of the SM, respectively. The experimental value of  $s_W$  results in a constraint that  $|\beta| \leq \sqrt{3}$ . The masses of the charged gauge bosons are

$$m_Y^2 = \frac{g^2}{4}(v_3^2 + v_1^2), \quad m_V^2 = \frac{g^2}{4}(v_3^2 + v_2^2), \quad m_W^2 = \frac{g^2}{4}(v_1^2 + v_2^2), \quad (5)$$

where the gauge boson  $W^\pm$  is identified with the SM one, implying that

$$v \equiv \sqrt{v_1^2 + v_2^2} = \frac{2m_W}{g} \simeq 246 \text{ GeV}. \quad (6)$$

The above Higgs sector is enough to generate all SM quark masses and heavy new quark masses [7–9]. Recall here that the Yukawa term  $Y_{3a}^u \overline{Q_{3L}} \rho^* u_{aR}$  generating the tree-level mass of top quark  $m_t \simeq \frac{Y_{33}^u v_2}{\sqrt{2}}$ , implying a lower bound  $t_\beta > 0.3$  corresponding to the perturbative limit of  $Y_{33}^u$ :  $s_\beta \geq \sqrt{2}m_t/(\sqrt{4\pi}v)$ , which is similar to the 2HDM type II [94].

The Higgs sector of the 331ISS( $K, K$ ) model is summarized in Appendix A, consisting of the singly charged Higgs part [14], other heavy charged Higgs used from notations of Refs. [7, 12]. The neutral Higgs sector consists of the SM-like Higgs boson inheriting properties consistent with experiments.

The model predicts three neutral gauge bosons including the massless photon. The relation between the original and physical bases of the neutral gauge bosons is

$$\begin{pmatrix} X_\mu \\ W_\mu^3 \\ W_\mu^8 \end{pmatrix} = \begin{pmatrix} s_{331}c_W, & (-s_{331}s_Wc_\theta + c_{331}s_\theta), & (s_{331}s_Ws_\theta + c_{331}c_\theta) \\ s_W, & c_Wc_\theta, & -s_\theta c_w \\ c_{331}c_W, & -(c_{331}s_Wc_\theta + s_{331}s_\theta), & (c_{331}s_Ws_\theta - s_{331}c_\theta) \end{pmatrix} \begin{pmatrix} A_\mu \\ Z_{1\mu} \\ Z_{2\mu} \end{pmatrix}, \quad (7)$$

where  $s_{331} \equiv \sin \theta_{331} = \sqrt{1 - \beta^2 t_W^2}$ ,  $c_{331} \equiv \cos \theta_{331} = \beta t_W$ , and  $t_X = \sqrt{6} t_W / s_{331}$ . In the limit  $v^2 / v_3^2 \rightarrow 0$ , the  $Z - Z'$  mixing angle  $\theta$  is [95]

$$s_\theta \equiv \sin \theta = \left( 3\beta t_W^2 + \frac{\sqrt{3}(t_\beta^2 - 1)}{t_\beta^2 + 1} \right) \frac{\sqrt{1 - \beta^2 t_W^2} v^2}{4c_W v_3^2}, \quad (8)$$

and  $M_{Z'}^2 = g^2 v_3^2 / (3s_{331}^2) + \mathcal{O}(v^2)$ . The lower  $SU(3)_L$  scale  $v_3$  of the  $331\beta$  model was indicated to be as large as the order  $\mathcal{O}(10)$  TeV [13, 96–100]. Hence, the neutral gauge bosons will be identified approximately as  $Z_2 \equiv Z'$  and  $Z_1 \equiv Z$  found experimentally.

The Yukawa Lagrangian is [14]

$$\begin{aligned} -\mathcal{L}_{\text{lepton}}^{\text{yuk}} = & \overline{e'_R} Y^e \eta^T L'_L + \overline{E'_R} Y^E \chi^T L'_L + \overline{\nu_R} Y^\nu \rho^T L'_L \\ & + \overline{\nu_R} M_R (X_R)^c + \frac{1}{2} \overline{X_R} \mu_X (X_R)^c + \overline{(X_R)^c} Y^h e'_R h^+ + \text{h.c.}, \end{aligned} \quad (9)$$

The perturbative limit of the matrix  $Y^h$  requires that  $|Y_{Ia}^h| < \sqrt{4\pi} \forall a = 1, 2, 3$  and  $I = \overline{1, K}$ . The symmetric matrix  $\mu_X$  is always chosen in the diagonal form  $\mu_X = \text{diag}(\mu_1, \mu_2, \dots, \mu_K)$  because of redefining the basis of  $X_R$  and  $M_R$ . We note that the general form of  $M_R$  can be diagonalized for determining the approximate form of the total neutrino mixing matrix [101]. In this work,  $M_R$  is transformed into the symmetric form, using a rotation redefining the two bases  $\nu_R$  and  $X_R$ , diagonalized generally through the following unitary transformations:

$$\begin{aligned} \mu_X & \rightarrow U_X^T \mu_X U_X = \text{diag}(\mu_1, \mu_2, \dots, \mu_K), \quad X_R \rightarrow X_R = U_X X_R, \\ M_R & \rightarrow M_R = M_R U_X^\dagger \rightarrow M_R = M_R^T = U_R M_R, \quad \nu_R \rightarrow \nu_R = U_R \nu_R. \end{aligned} \quad (10)$$

Therefore, we will work with assumptions that  $\mu_X$  is diagonal and  $M_R$  is symmetric,  $M_R = M_R^T$ , leading to the unitary transformation  $U_N$  into the diagonal form  $\hat{M}_R$ :

$$U_N^T M_R U_N = \hat{M}_R = \text{diag}(M_1, M_2, \dots, M_K). \quad (11)$$

In the Lagrangian (9), the neutrino Dirac mass matrix comes from the third term including the Higgs triplet  $\rho$  which also generates the top quark mass. The Dirac mass term and the Yukawa couplings  $Y^h$  depend on  $t_\beta$  differently from those mentioned in Ref. [102]. The lepton mass terms are

$$-\mathcal{L}_{\text{lepton}}^{\text{mass}} = \frac{Y_{ab}^e v_1}{\sqrt{2}} \overline{e'_{aR}} e'_{bL} + \frac{Y_{ab}^E v_3}{\sqrt{2}} \overline{E'_{aR}} E'_{bL} + \frac{1}{2} \left( \overline{(\nu'_L)^c} \quad \overline{\nu_R} \quad \overline{X_R} \right) \mathcal{M}^\nu \begin{pmatrix} \nu'_L \\ (\nu_R)^c \\ (X_R)^c \end{pmatrix} + \text{h.c.},$$

$$\mathcal{M}^\nu = \begin{pmatrix} \mathcal{O}_{3 \times 3} & m_D^T & \mathcal{O}_{3 \times K} \\ m_D & \mathcal{O}_{K \times K} & M_R^T \\ \mathcal{O}_{K \times 3} & M_R & \mu_X \end{pmatrix}, \quad (12)$$

where  $(m_D)_{Ib} \equiv m_{D,Ib} = -\frac{Y_{Ib}^\nu v_2}{\sqrt{2}}$  for all  $I = \overline{1, K}$ , and

$$\nu'_L = (\nu'_1, \nu'_2, \nu'_3)_L^T, \quad \nu_R = (\nu_1, \nu_2, \dots, \nu_K)_R^T, \quad X_R = (X_1, X_2, \dots, X_K)_R^T.$$

The total mixing matrix is defined as

$$U^{\nu T} \mathcal{M}^\nu U^\nu = \hat{\mathcal{M}}^\nu = \text{diag}(m_{n_1}, m_{n_2}, \dots, m_{n_{2K+3}}),$$

$$\begin{pmatrix} \nu'_L \\ (\nu_R)^c \\ (X_R)^c \end{pmatrix} = U^\nu n_L, \quad \begin{pmatrix} (\nu'_L)^c \\ \nu_R \\ X_R \end{pmatrix} = U^{\nu*} n_R = U^{\nu*} (n_L)^c, \quad (13)$$

where  $n_{L,R} = (n_1, n_2, \dots, n_{2K+3})_{L,R}$  are Majorana neutrino mass eigenstates  $n_{iL,R} = (n_{iR,L})^c$ .

In this work, we will consider the general case in which the flavor charged leptons are not physical, i.e. left and right  $3 \times 3$  unitary matrices  $U_{L(R)}^e$  and  $V_{L(R)}^E$  used to change into the mass eigenstates of SM and heavy leptons are defined as follows:

$$e'_{L(R)} = U_{L(R)}^e e_{L(R)}, \quad U_R^{e\dagger} Y^e U_L^e = \frac{\sqrt{2}}{v_1} \hat{m}_\ell = \frac{\sqrt{2}}{v_1} \text{diag}(m_e, m_\mu, m_\tau) \quad (14)$$

$$E'_{aL(R)} = (V_{L(R)}^E)_{ab} E_{bL(R)}, \quad V_R^{E\dagger} Y^E V_L^E = \frac{\sqrt{2}}{v_3} \hat{m}_E = \frac{\sqrt{2}}{v_3} \text{diag}(m_{E_1}, m_{E_2}, m_{E_3}). \quad (15)$$

The total neutrino mixing matrix is parameterized in the seesaw form

$$U^\nu = \begin{pmatrix} (I_3 - \frac{1}{2} R R^\dagger) U_3^\nu & R V_N \\ -R^\dagger U_3^\nu & (I_{2K} - \frac{1}{2} R^\dagger R) V_N \end{pmatrix} + \mathcal{O}(R^3), \quad (16)$$

where  $V_N$  is a  $2K \times 2K$  unitary matrix;  $R$  is a  $3 \times 2K$  matrix satisfying  $|R_{aI}| < 1$  for all  $a = 1, 2, 3$ , and  $I = 1, 2, \dots, 2K$ . The  $3 \times 3$  unitary matrix  $U_{\text{PMNS}}$  is the Pontecorvo-Maki-Nakagawa-Sakata (PMNS) matrix, defined as

$$U_{\text{PMNS}} \equiv U_L^{e\dagger} U_3^\nu \rightarrow U_3^\nu = U_L^e U_{\text{PMNS}}. \quad (17)$$

Now, the Dirac and Majorana mass matrices have well-known ISS forms as [103, 104]

$$M_D^T = (m_D^T, \quad \mathcal{O}_{3 \times K}), \quad M_N = \begin{pmatrix} \mathcal{O}_{K \times K} & M_R \\ M_R^T & \mu_X \end{pmatrix}, \quad (18)$$

and both  $M_R$  and  $\mu_X$  are  $K \times K$  matrices. The condition  $\max|R_{ij}| \equiv ||R|| \ll 1$  gives the ISS relations approximately as follows:

$$R = \left( \mathcal{O}_{3 \times K}, \quad m_D^\dagger \left( M_R^\dagger \right)^{-1} \right), \quad (19)$$

$$\hat{m}_\nu = U_3^{\nu T} m_\nu U_3^\nu = U_3^{\nu T} m_D^T \left( M_R^T \right)^{-1} \mu_X M_R^{-1} m_D U_3^\nu, \quad (20)$$

$$V_N^* \hat{M}_N V_N^\dagger \simeq M_N. \quad (21)$$

A general parametrization of  $m_D$  is based on Eq. (20) [105], using a  $K \times 3$  matrix  $\xi$  defined as  $\xi \equiv \mu_X^{\frac{1}{2}} M_R^{-1} m_D U_3^\nu \hat{m}_\nu^{-\frac{1}{2}}$ , which obeys the orthogonal relation  $\xi^T \xi = I_3$  when all active neutrinos are massive. On the other hand, in the mISS framework consisting of a massless neutrino, the formula of  $\hat{m}_\nu^{-\frac{1}{2}}$  needs to be defined as

$$\hat{m}_\nu^{-\frac{1}{2}} \equiv \begin{cases} \text{diag} \left( 0, m_{n_2}^{-\frac{1}{2}}, m_{n_3}^{-\frac{1}{2}} \right) & \text{(NO)} \\ \text{diag} \left( m_{n_1}^{-\frac{1}{2}}, m_{n_2}^{-\frac{1}{2}}, 0 \right) & \text{(IO)} \end{cases}, \quad (22)$$

which satisfies  $\xi^T \xi = \text{diag}(0, 1, 1)$  (NO) or  $\xi^T \xi = \text{diag}(1, 1, 0)$  (IO). The NO and IO schemes are defined as two different ways of arranging the active neutrino masses that  $m_{n_1} < m_{n_2} < m_{n_3}$  and  $m_{n_3} < m_{n_1} < m_{n_2}$ , respectively.

The analytic form of  $m_D$  is derived generally as follows

$$m_D = x_0^{\frac{1}{2}} M_R \hat{\mu}_X^{-\frac{1}{2}} \xi \hat{x}_\nu^{\frac{1}{2}} U_3^{\nu \dagger}, \\ R \simeq (\mathcal{O}_{3 \times K}, R_0), \quad R_0 \equiv x_0^{\frac{1}{2}} U_3^\nu \hat{x}_\nu^{\frac{1}{2}} \xi^\dagger \hat{\mu}_X^{-\frac{1}{2}}, \quad (23)$$

where  $x_0$  is defined as the ratio of the two scales of  $\mu_X$  and active neutrino masses, namely:

$$x_0 \equiv \frac{\max[m_{n_1}, m_{n_2}, m_{n_3}]}{\max[|(\mu_X)_{11,22}|]} \ll 1, \\ \hat{\mu}_X \equiv \frac{\mu_X}{\max[|(\mu_X)_{11,22}|]}, \quad \hat{x}_\nu \equiv \frac{\hat{m}_\nu}{\max[m_{n_1}, m_{n_2}, m_{n_3}]}. \quad (24)$$

The ISS condition  $|\hat{m}_\nu| \ll |\mu_X| \ll |m_D| \ll M_{1,2}$  gives  $\frac{\sqrt{\mu_X \hat{m}_\nu}}{M_{1,2}} \simeq 0$  and  $x_0 \ll 1$  but nonzero, which can be considered as the nonunitary scale of the active neutrino mixing matrix.

In the specific mISS framework consisting of one active massless neutrino, the matrix  $\xi$  with all real entries is shown to have only the form

$$\xi(\text{NO}) = \begin{pmatrix} 0 & c_\phi & -s_\phi \\ 0 & s_\phi & c_\phi \end{pmatrix}, \quad \xi(\text{IO}) = \begin{pmatrix} c_\phi & -s_\phi & 0 \\ s_\phi & c_\phi & 0 \end{pmatrix}, \quad (25)$$

where  $c_\phi \equiv \cos \phi$  and  $s_\phi \equiv \sin \phi$ .

Based on Eqs. (11) and (21), we derive that

$$\hat{M}_N = \begin{pmatrix} \hat{M}_R & \mathcal{O}_{K \times K} \\ \mathcal{O}_{K \times K} & \hat{M}_R \end{pmatrix}, \quad V_N \simeq \frac{1}{\sqrt{2}} \begin{pmatrix} -iU_N & U_N \\ iU_N & U_N \end{pmatrix}. \quad (26)$$

Consequently, the approximate formula of  $U^\nu$  ignoring the  $\mathcal{O}(|R_0|^3)$  part is

$$U^\nu \simeq \begin{pmatrix} \left( I_3 - \frac{R_0 R_0^\dagger}{2} \right) U_3^\nu & \frac{iR_0 U_N}{\sqrt{2}} & \frac{R_0 U_N}{\sqrt{2}} \\ \mathcal{O}_{K \times 3} & -\frac{iU_N}{\sqrt{2}} & \frac{U_N}{\sqrt{2}} \\ -R_0^\dagger U_3^\nu & \left( I_K - \frac{R_0^\dagger R_0}{2} \right) \frac{iU_N}{\sqrt{2}} & \left( I_K - \frac{R_0^\dagger R_0}{2} \right) \frac{U_N}{\sqrt{2}} \end{pmatrix} \equiv \begin{pmatrix} U_0^\nu \\ U_1^\nu \\ U_2^\nu \end{pmatrix}, \quad (27)$$

where  $U_k^\nu$  with  $k = 0, 1, 2$  used for derivation the Higgs couplings with leptons.

The simplest case of  $m_D$  is  $m_D = x_0^{\frac{1}{2}} \hat{M}_R \hat{x}_\nu^{\frac{1}{2}} U_{\text{PMNS}}^\dagger$  with  $\mu_X = \mu_X I_K$ ,  $U_{L(R)}^e = I_3$ , and  $M_R \equiv \hat{M}_R = M_0 I_K$ . Consequently, formulas of  $m_D$  and  $R$  with the simplest form of  $\xi$  are

$$m_D = x_0^{\frac{1}{2}} \hat{M}_R \hat{x}_\nu^{\frac{1}{2}} U_{\text{PMNS}}^\dagger, \quad R \simeq \left( \mathcal{O}_{3 \times K}, x_0^{\frac{1}{2}} U_{\text{PMNS}} \hat{x}_\nu^{\frac{1}{2}} \right), \quad (28)$$

which is the most popular form used to discuss on the LFV processes for standard ISS model with  $K = 3$ . Using the ISS relation, the total neutrino mixing matrix given in Eq. (16) are determined approximately from  $V$  and  $R$  given in Eqs. (26) and (28), respectively. We will see below that this simple form in the mISS framework cannot explain the  $1\sigma$  experimental  $(g-2)_\mu$  data because there appears a strict correlation with the decay rate  $\text{Br}(\tau \rightarrow \mu\gamma)$  so that the experimental constraint results an upper bound on  $\Delta a_{\mu,e}$ .

### III. COUPLINGS AND LFV ANALYTICAL FORMULAS

#### A. LFV sources and $(g-2)_{e_a}$ anomalies

All vertices relating to couplings of singly charged Higgs bosons that give one-loop contributions to  $e_b \rightarrow e_a \gamma$  decay rates and  $a_{e_a}$  anomalies are collected from the Lagrangian (9). Namely, the relevant part in terms of physical lepton states is

$$\begin{aligned} \mathcal{L}_{\text{lep}}^Y = & -\bar{e}_R \frac{\sqrt{2}\hat{m}_\ell}{v_1} \left[ e_L \eta^0 + U_L^{e\dagger} U_0^\nu n_L (-\eta^-) + U_L^{e\dagger} V_L^E E_L \eta^{-A} \right] \\ & -\bar{E}_R \frac{\sqrt{2}\hat{m}_E}{v_3} \left[ V_L^{E\dagger} U_L^e e_L \chi^A + V_L^{E\dagger} U_0^\nu n_L (-\chi^{-B}) + E_L \chi^0 \right] \end{aligned}$$

$$\begin{aligned}
& -\bar{n}_R \left( \frac{-\sqrt{2}}{v_2} \right) U_1^{\nu T} m_D [U_L^e e_L \rho^+ + U_0^\nu n_L (-\rho^0) + V_L^E E_L \rho^{-B}] \\
& -\bar{n}_L U_2^{\nu \dagger} Y^h U_R^e e_R h^+ + \text{h.c.} + \dots,
\end{aligned} \tag{29}$$

where  $\psi_{L(R)} = (\psi_1, \psi_2, \psi_3)_{L(R)}^T$  with  $\psi = e, E$ . In the physical base of Higgs and gauge bosons, Eq. (29) is

$$\begin{aligned}
\mathcal{L}_{\text{lep}}^Y = & -\frac{g}{\sqrt{2}m_W} \sum_{k=1}^2 \sum_{a=1}^3 \sum_{i=1}^{3+2K} \bar{n}_i \left[ \lambda_{ia}^{L,k} P_L + \lambda_{ia}^{R,k} P_R \right] e_a H_k^+ \\
& -\frac{g}{\sqrt{2}m_Y} \sum_{a,c=1}^3 V_{ac}^{L*} \bar{E}_c \left[ m_{E_c} t_{13} P_L + \frac{m_{e_a}}{t_{13}} P_R \right] e_a H^A \\
& + \sum_{a=1}^3 \sum_{i=1}^{3+2K} \frac{g}{\sqrt{2}} \left( U_1^{\nu \dagger} U_L^e \right)_{ia} \bar{n}_i \gamma^\mu P_L e_a W_\mu^+ \\
& + \sum_{a,c=1}^3 \frac{g}{\sqrt{2}} \left( V_L^{E \dagger} U_L^e \right)_{ca} \bar{E}_c \gamma^\mu P_L e_a Y_\mu^A + \text{h.c.},
\end{aligned} \tag{30}$$

where  $t_{13}$  is defined in Eq. (A5) and  $\lambda_{i,a}^{L(R),k}$  calculated from  $U^\nu$  in Eq. (27) are

$$\begin{aligned}
\lambda_{ia}^{L,1} &= -t_\beta^{-1} c_\alpha \left( U_1^{\nu T} m_D U_L^e \right)_{ia} \\
&\simeq \frac{t_\beta^{-1} c_\alpha}{\sqrt{2}} \times \begin{cases} 0, & i \leq 3 \\ i x_0^{\frac{1}{2}} \left( U_{\text{PMNS}}^* \hat{x}_\nu^{\frac{1}{2}} \xi^T \hat{\mu}_X^{-\frac{1}{2}} U_N^* \hat{M}_R \right)_{a(i-3)}, & 0 < i-3 \leq K \\ -x_0^{\frac{1}{2}} \left( U_{\text{PMNS}}^* \hat{x}_\nu^{\frac{1}{2}} \xi^T \hat{\mu}_X^{-\frac{1}{2}} U_N^* \hat{M}_R \right)_{a(i-3-K)}, & K < i-3 \leq 2K \end{cases}, \\
\lambda_{ia}^{L,2} &\simeq \lambda_{ia}^{L,1} t_\alpha, \\
\lambda_{ia}^{R,1} &= -t_\beta m_a c_\alpha \left( U_0^{\nu \dagger} U_L^e \right)_{ia} - \frac{v s_\alpha}{\sqrt{2}} \left( U_2^{\nu \dagger} Y^h U_R^e \right)_{ia} \\
&\simeq \begin{cases} -m_a t_\beta c_\alpha \left( U_{\text{PMNS}}^\dagger \right)_{ia} + \frac{v s_\alpha}{\sqrt{2}} \left( x_0^{\frac{1}{2}} \hat{x}_\nu^{\frac{1}{2}} \xi^\dagger \hat{\mu}_X^{-\frac{1}{2}} Y^h U_R^e \right)_{ia}, & i \leq 3 \\ \frac{i\sqrt{x_0}}{\sqrt{2}} m_a t_\beta c_\alpha \left( U_N^\dagger \hat{\mu}_X^{-\frac{1}{2}} \xi \hat{x}_\nu^{\frac{1}{2}} U_{\text{PMNS}}^\dagger \right)_{(i-3)a} + \frac{i v s_\alpha}{2} \left( U_N^\dagger Y^h U_R^e \right)_{(i-3)a}, & 0 < i-3 \leq K \\ -\frac{\sqrt{x_0}}{\sqrt{2}} m_a t_\beta c_\alpha \left( U_N^\dagger \hat{\mu}_X^{-\frac{1}{2}} \xi \hat{x}_\nu^{\frac{1}{2}} U_{\text{PMNS}}^\dagger \right)_{(i-3-K)a} - \frac{v s_\alpha}{2} \left( U_N^\dagger Y^h U_R^e \right)_{(i-3-K)a}, & K < i-3 \leq 2K \end{cases}, \\
\lambda_{ia}^{R,2} &= \lambda_{ia}^{R,1} [c_\alpha \rightarrow s_\alpha, s_\alpha \rightarrow -c_\alpha],
\end{aligned} \tag{31}$$

For convenience to estimate the dominant one-loop contributions to  $\Delta a_{e_a}$ , parts proportional to  $x_0$  are ignored; see a detailed calculation with  $K = 3$  in Refs. [14, 106].

The form factors  $c_{(ab)R}^X$  relating to new one-loop contributions from exchanging the  $X$  boson to the  $\Delta a_{e_a}$  and cLFV decays were introduced in Ref. [107]. Formulas of  $c_{(ab)R}^X$  with

$X = H^A, W^\pm, Y^{\pm A}$  were introduced precisely in Ref. [14] for the general seesaw scheme, consistent with those discussed in Ref. [12]. It was shown previously that  $c_{(22)R}^X \ll \Delta a_\mu^{\text{NP}}$  with  $X = H^A, Y$  [14]; we therefore fix  $c_{(ab)R}^X = 0$  by a simple assumption that  $m_{E_a} \equiv m_E \forall a = 1, 2, 3$ , and  $V_{L,R}^E = I_3$ . The contributions from singly charged Higgs and  $W$  bosons are

$$\begin{aligned}
c_{(ab)R}(H_k^\pm) &= \frac{g^2 e}{32\pi^2 m_W^2 m_{H_k^\pm}^2} \\
&\quad \times \sum_{i=1}^{3+2K} \left[ \lambda_{ia}^{L,k*} \lambda_{ib}^{R,k} m_{n_i} f_\Phi(t_{i,k}) + \left( m_b \lambda_{ia}^{L,k*} \lambda_{ib}^{L,k} + m_a \lambda_{ia}^{R,k*} \lambda_{ib}^{R,k} \right) \tilde{f}_\Phi(t_{i,k}) \right], \\
c_{(ab)R}(H^\pm) &= \sum_{k=1}^2 c_{(ab)R}(H_k^\pm), \\
c_{(ab)R}(W) &\simeq \frac{e G_F m_b}{4\sqrt{2}\pi^2} \left\{ -\frac{5}{12} \left[ \delta_{ab} - x_0 \left( U_{\text{PMNS}} \hat{x}_\nu^{\frac{1}{2}} \xi^\dagger \hat{\mu}_X^{-1} \xi \hat{x}_\nu^{\frac{1}{2}} U_{\text{PMNS}}^\dagger \right)_{ab} \right] \right. \\
&\quad \left. + x_0 \sum_{I=1}^K \left( U_{\text{PMNS}} \hat{x}_\nu^{\frac{1}{2}} \xi^\dagger \hat{\mu}_X^{-\frac{1}{2}} U_N \right)_{aI} \left( U_N^\dagger \hat{\mu}_X^{-\frac{1}{2}} \xi \hat{x}_\nu^{\frac{1}{2}} U_{\text{PMNS}}^\dagger \right)_{Ib} \tilde{f}_V(x_{I,W}) \right\}, \tag{32}
\end{aligned}$$

where  $t_{i,k} \equiv m_{n_i}^2/m_{H_k^\pm}^2$ ,  $x_{I,W} \equiv M_I^2/m_W^2$ ;  $U_{\text{PMNS}}$  was defined in Eq. (17), and the functions  $f_\Phi(x)$ ,  $\tilde{f}_\Phi(x)$ , and  $\tilde{f}_V(x)$  are given in Appendix B. We comment here that  $c_{(ab)R}(W)$  consist of two parts, in which the first part proportional to  $\delta_{ab}$  is exactly the SM results, and this first part does not contribute to LFV decay. In contrast, the second part has a factor  $x_0 \ll 1$ ; therefore this part gives small contribution to  $\Delta a_{e_a}$ , but still significantly affects to  $\text{Br}(\mu \rightarrow e\gamma)$  under the current experimental constraint. Therefore, we still add this part in the numerical investigation. In this work, we use the limit  $m_{n_i} = 0$  with  $i = 1, 2, 3$ ;  $m_{n_{3+I}} = m_{n_{3+K+I}} = M_I \forall I = \overline{1, K}$ . The dominant contribution to  $\Delta a_{e_a}$  is

$$c_{(ab)R,0}(H_k^\pm) = \frac{g^2 e v t_\beta^{-1} c_\alpha s_\alpha x_0^{\frac{1}{2}}}{32\sqrt{2}\pi^2 m_W^2} \sum_{I=1}^K \left[ \left( U_{\text{PMNS}} \hat{x}_\nu^{1/2} \xi^\dagger \hat{\mu}_X^{-1/2} U_N \hat{M}_R \right)_{aI} \left( U_N^\dagger Y^h U_R^e \right)_{Ib} \frac{x_{I,k} f_\Phi(x_{I,k})}{M_I} \right],$$

where  $U_R^e$  was defined in Eq. (14);  $x_{I,k} \equiv M_I^2/m_{H_k^\pm}^2$  for  $k = 1, 2$ ; and  $I = \overline{1, K}$ . Consequently, the dominant contribution from the sum of the two singly charged Higgs bosons to  $\Delta a_{e_a}$  [ $\text{Br}(e_b \rightarrow e_a\gamma)$ ] when  $a = b$  ( $a \neq b$ ) is

$$c_{(ab)R,0}(H^\pm) = \frac{g^2 e}{32\pi^2 m_W^2} \left[ \frac{v t_\beta^{-1} x_0^{\frac{1}{2}} c_\alpha s_\alpha}{\sqrt{2}} \left( U_{\text{PMNS}} \hat{x}_\nu^{1/2} \xi^\dagger \hat{\mu}_X^{-1/2} U_N \hat{F} U_N^\dagger Y^h U_R^e \right)_{ab} \right], \tag{33}$$

$$\hat{F} \equiv \text{diag} \left( \hat{F}_1, \hat{F}_2, \dots, \hat{F}_K \right),$$

$$\hat{F}_I = \sum_{k=1}^2 (-1)^{k-1} x_{I,k} f_{\Phi}(x_{I,k}) = x_{I,1} f_{\Phi}(x_{I,1}) - x_{I,2} f_{\Phi}(x_{I,2}). \quad (34)$$

We emphasize that Eq. (33) is the most general form, including the mixing matrices of charged and neutral leptons  $e_a$  and  $n_i$ , and consistent with the result given in Ref. [14] with  $K = 3$ ,  $U_L^e = U_R^e = U_N = \xi = I_3$ , and  $M_I = M_0 \forall I = \overline{1, K}$ . Equation (33) is very important for estimating analytic relations to cancel the large contributions to  $\text{Br}(e_b \rightarrow e_a \gamma)$  consistent with experiments, while keeping the large  $\Delta a_{e,\mu}$ . The numerical scanning time to determine the allowed points reduce dramatically.

The one-loop contribution of  $X = H_{1,2}^{\pm}, H^A, W, Y$  to  $\Delta a_{e_a}$  is  $a_{e_a}(X) = -\frac{4m_a}{e} \text{Re} [c_{(aa)R}(X)]$ , leading to a deviation from the SM as

$$\Delta a_{e_a} = \sum_X a_{e_a}(X) - a_{e_a}^{\text{SM}}(W) \simeq -\frac{4m_a}{e} \text{Re} [c_{(aa)R}(H^{\pm})], \quad (35)$$

where  $a_{e_a}^{\text{SM}}(W)$  is the one-loop contributions of  $W$  boson predicted by the SM. The heavy neutral Higgs and gauge bosons give suppressed one-loop contributions to  $\Delta a_{e_a}$  [14], so we omit them here.

## B. One-loop contributions to LFV decays

From the information shown in Eqs. (29) and (30), we obtain all vertices needed for the calculations all one-loop contributions to  $e_b \rightarrow e_a \gamma$  in the unitary gauge, consistent with Refs. [12, 14]. They are listed in Table I, following conventions for general Lagrangian parts to derive these Feynman rules given in Appendix C. In the  $331\beta$  model, the two first components of the Higgs triplets can play roles of those appearing in the 2HDM; see a detailed discussion in Ref. [9], for example. As a result, many available properties of the Higgs couplings and masses from the 2HDM model are valid in the  $331\beta$  model framework. On the other hand, there are  $SU(3)_L$  particles such as  $H^A, Y^A$ , and heavy charged leptons  $E_a$  having masses in the  $SU(3)_L$  scale  $v_3$ . Studies of searching for them in colliders were discussed in Refs. [154–156], which suggest promising signals in the future colliders if they exist. Note that in the  $331\beta$  the  $SU(3)_L$  particles may carry exotic electric charges, implying the existence of long-lived exotic charged particles being searched for at the LHC [157]. Discussions for some particular channels relating to the  $SU(3)_L$  lepton searches in 3-3-1 models are given in Refs.

Vertex	Coupling	Vertex	Coupling
$\bar{n}_i e_a H_k^+$	$-\frac{ig}{\sqrt{2}m_W} \left( \lambda_{ia}^{L,k} P_L + \lambda_{ia}^{R,k} P_R \right)$	$\bar{e}_a n_i H_k^-$	$-\frac{ig}{\sqrt{2}m_W} \left( \lambda_{ia}^{R,k*} P_L + \lambda_{ia}^{L,k*} P_R \right)$
$\bar{E}_c e_a H^{+A}$	$\frac{-ig(V_L^{E\dagger} U_L^e)_{ca}}{\sqrt{2}m_Y} \left( m_{E_c} t_{13} P_L + \frac{m_a}{t_{13}} P_R \right)$	$\bar{e}_a E_c H^{-A}$	$\frac{-ig(V_L^{E\dagger} U_L^e)_{ca}^*}{\sqrt{2}m_Y} \left( \frac{m_a}{t_{13}} P_L + m_{E_c} t_{13} P_R \right)$
$\bar{n}_i e_a W^{+\mu}$	$\frac{ig}{\sqrt{2}} (U_0^{\nu\dagger} U_L^e)_{ia} \gamma_\mu P_L$	$\bar{e}_a n_i W^{-\mu}$	$\frac{ig}{\sqrt{2}} (U_0^{\nu\dagger} U_L^e)_{ia}^* \gamma_\mu P_L$
$\bar{E}_c e_a Y^{+A\mu}$	$\frac{ig(V_L^{E\dagger} U_L^e)_{ca}}{\sqrt{2}} \gamma_\mu P_L$	$\bar{e}_a E_c Y^{-A\mu}$	$\frac{ig(V_L^{E\dagger} U_L^e)_{ca}^*}{\sqrt{2}} \gamma_\mu P_L$
$A^\lambda W^{+\mu} W^{-\nu}$	$-ie\Gamma_{\lambda\mu\nu}(p_0, p_+, p_-)$	$A^\lambda Y^{+A\mu} Y^{-A\nu}$	$-ieA\Gamma_{\lambda\mu\nu}(p_0, p_+, p_-)$
$A^\mu H_k^+ H_k^-$	$ie(p_+ - p_-)_\mu$	$A^\mu H^{+A} H^{-A}$	$ieA(p_+ - p_-)_\mu$
$A^\mu \bar{e}_a e_a$	$-ie\gamma_\mu$	$A^\mu \bar{E}_a E_a$	$ieB\gamma_\mu$

TABLE I. Feynman rules for cLFV decays  $e_b \rightarrow e_a \gamma$  in the 331 $\beta$ ISS( $K, K$ ) model,  $k = 1, 2$ .

[13, 158–160]. Constraints of lower bounds for these lepton masses are at least 600 GeV for charged leptons  $E_a$  [161, 162]. The lower bound of  $v_3$  was derived the most strictly from studying the production and decay of the heavy neutral gauge boson  $Z'$  at the LHC and future colliders. Consequently, the mass of the gauge boson  $Y$  must be of the order of TeV; therefore this boson gives suppressed one-loop contributions to the LFV decay amplitudes under consideration.

Here we use the general results given in Refs. [12, 107, 108] in the limit of heavy charged Higgs and gauge bosons, while tiny neutrino masses are still allowed. The cLFV decays  $e_b \rightarrow e_a \gamma$  will be used to constrain the parameter space of the model. The contributions to the decay rates are derived from the couplings and Feynman rules given in Table I, namely,

$$\text{Br}(e_b \rightarrow e_a \gamma) = \frac{48\pi^2}{m_b^2 G_F^2} \left( |c_{(ab)R}|^2 + |c_{(ba)R}|^2 \right) \text{Br}(e_b \rightarrow e_a \bar{\nu}_a \nu_b), \quad (36)$$

where  $G_F = g^2/(4\sqrt{2}m_W^2)$ , and

$$c_{(ab)R} = c_{(ab)R}(W) + c_{(ab)R}(Y) + c_{(ab)R}(H^\pm) + c_{(ab)R}(H^A). \quad (37)$$

Apart from Table I, the couplings for one-loop contributions to the LFV $h$  decays  $h \rightarrow e_a e_b$  are listed as the following.

From the above discussion on the Higgs potential, we can derive all Higgs self-couplings of the SM-like Higgs boson using the interacting Lagrangian

$$\mathcal{L}_{hHH} = -V_h = \sum_{s_1 s_2} \left( -\lambda_{hs_1 s_2} h s_1^Q s_2^{-Q} + \text{h.c.} \right) + \dots$$

The Feynman rule for a vertex  $hs_1^Q s_2^{-Q}$  is  $(-i\lambda_{hs_1 s_2})$ , where  $s_1, s_2 = H_{1,2}^\pm, H^{\pm A}$  and

$$\begin{aligned}
\lambda_{hH_1^+ H_1^-} &= 2c_\alpha^2 c_\beta c_\zeta \lambda_1 s_\beta^2 v - 2c_\alpha^2 c_\beta^2 \lambda_2 s_\beta s_\zeta v + c_\alpha^2 \lambda_{12} v (c_\beta^3 c_\zeta - s_\beta^3 s_\zeta) + c_\alpha^2 c_\delta \tilde{\lambda}_{12} v \\
&\quad + s_\alpha^2 v (c_\beta c_\zeta \lambda_2^h - s_\beta s_\zeta \lambda_1^h) - \sqrt{2} c_\alpha c_\delta f_h s_\alpha, \\
\lambda_{hH_2^+ H_2^-} &= 2c_\beta s_\alpha^2 s_\beta v (c_\zeta \lambda_1 s_\beta - c_\beta \lambda_2 s_\zeta) + \lambda_{12} s_\alpha^2 v (c_\beta^3 c_\zeta - s_\beta^3 s_\zeta) + c_\delta \tilde{\lambda}_{12} s_\alpha^2 v \\
&\quad + c_\alpha^2 v (c_\beta c_\zeta \lambda_2^h - s_\beta s_\zeta \lambda_1^h) + \sqrt{2} c_\alpha c_\delta f_h s_\alpha, \\
\lambda_{hH_1^\pm H_2^\mp} &= 2c_\alpha c_\beta s_\alpha s_\beta v (c_\zeta \lambda_1 s_\beta - c_\beta \lambda_2 s_\zeta) + c_\alpha \lambda_{12} s_\alpha v (c_\beta^3 c_\zeta - s_\beta^3 s_\zeta) + c_\alpha c_\delta \tilde{\lambda}_{12} s_\alpha v \\
&\quad + c_\alpha s_\alpha v (s_\beta s_\zeta \lambda_1^h - c_\beta c_\zeta \lambda_2^h) + \frac{c_\delta f_h (c_\alpha^2 - s_\alpha^2)}{\sqrt{2}}, \\
\lambda_{hH^A H^{-A}} &= c_{13}^2 v (2c_\beta c_\zeta \lambda_1 - \lambda_{12} s_\beta s_\zeta) + s_{13}^2 v (c_\beta c_\zeta \lambda_{13} - \lambda_{23} s_\beta s_\zeta) + c_\zeta \tilde{\lambda}_{13} s_{13} (c_{13} v_3 + c_\beta s_{13} v) \\
&\quad + 2f c_{13} s_{13} s_\zeta.
\end{aligned} \tag{38}$$

The couplings of Higgs and gauge bosons are contained in the covariant kinetic terms of the Higgs bosons. From general notations discussed in Appendix C, the Feynman rules for particular couplings relating to SM-like Higgs boson are derived using the vertex factors shown in Table II, which is consistent with Ref. [8] in the limit  $\alpha = 0$ . The  $H_k^\pm h W^\mp$

Vertex	Coupling:	Vertex	Coupling
$g_{hW^+W^-}$	$g m_W c_\delta$		
$g_{hH_2^- W^+}$	$-\frac{g c_\alpha s_\delta}{2}$	$g_{hH_1^- W^+}$	$-\frac{g s_\alpha s_\delta}{2}$
$g_{hY^+ A Y^- A}$	$g m_W c_\beta c_\zeta$	$g_{hH^- A Y^+ A}$	$-\frac{g c_{13} c_\zeta}{2}$

TABLE II. Vertex factors for SM-like Higgs couplings to charged Higgs and gauge bosons in the 331 $\beta$ ISS( $K, K$ ) model.

couplings with  $k=1,2$  always consist of the suppressed factor  $s_\delta \ll 1$ , which has the same property known in 2HDM. In particular,  $s_\delta = 0$  is the aligned limit to guarantee that the SM-like Higgs couplings are consistent with the SM prediction. The small  $s_\delta$  is also consistent with the nonobservations of  $H_1^\pm$  through the decay channel search  $H^\pm \rightarrow hW^\pm$  at the LHC. Therefore, we can ignore the relevant one-loop contributions to the LFV $h$  decay amplitudes  $h \rightarrow e_a e_b$  in numerical investigations.

Similarly, for the one-loop contributions to the decay  $Z \rightarrow e_b^+ e_a^-$ , the needed couplings are given in Ref. [8]; see Table III. Because  $g_{ZW^+ H_1^-} \propto s_\theta = \mathcal{O}(v^2/v_3^2) \leq \mathcal{O}(10^{-4})$ , one-loop contributions to LFV $Z$  amplitudes relating to  $ZW^\pm H_k^\mp$  are suppressed.

Vertex	Coupling	
$g_{ZH_1^+ H_1^-}$	$\frac{1}{2c_W s_W}$	$c_\theta (c_\alpha^2 - 2s_W^2) + \frac{c_W s_\theta (c_\alpha^2 (2\sqrt{3}s_\beta^2 + 3\beta t_W^2 - \sqrt{3}) + 6\beta s_\alpha^2 t_W^2)}{3\sqrt{1-\beta^2 t_W^2}}$
$g_{ZH_2^+ H_2^-}$	$\frac{1}{2s_W c_W}$	$c_\theta (s_\alpha^2 - 2s_W^2) + \frac{c_W s_\theta (6\beta c_\alpha^2 t_W^2 + s_\alpha^2 (2\sqrt{3}s_\beta^2 + 3\beta t_W^2 - \sqrt{3}))}{3\sqrt{1-\beta^2 t_W^2}}$
$g_{ZH_{1(2)}^+ H_{2(1)}^-}$	$\frac{s_\alpha c_\alpha}{2s_W c_W}$	$c_\theta - \frac{c_W s_\theta (-2\sqrt{3}s_\beta^2 + 3\beta t_W^2 + \sqrt{3})}{3\sqrt{1-\beta^2 t_W^2}}$
$g_{ZH^A H^{-A}}$	$\frac{1}{2s_W c_W}$	$\left( c_\theta [s_{13}^2 - (1 + \sqrt{3}\beta)s_W^2] + \frac{s_\theta [\sqrt{3}c_W^2 (s_{13}^2 - 2) + 3\beta(\sqrt{3}\beta + c_{13}^2)s_W^2]}{3c_W \sqrt{1-\beta^2 t_W^2}} \right)$
$g_{ZW^+ H_1^-}$		$-\frac{2c_\alpha c_\beta m_W s_\beta s_\theta}{s_W \sqrt{3-3\beta^2 t_W^2}}$
$g_{ZW^+ H_2^-}$		$-\frac{2c_\alpha c_\beta m_W s_\beta s_\theta}{2s_W \sqrt{3-3\beta^2 t_W^2}}$
$g_{ZY^A H^{-A}}$		$\frac{g c_{13}}{4s_W} \left\{ c_\theta c_W [s_{12} (1 + (2 + \sqrt{3}\beta)t_W^2) v + t_{13} (1 - \sqrt{3}\beta t_W^2) v_3] \right.$ $\left. + \frac{s_\theta}{3\sqrt{1-\beta^2 t_W^2}} [s_{12} (\sqrt{3} - 3\beta(2 + \sqrt{3}\beta)t_W^2) v + \sqrt{3}t_{13} (1 + 3\beta^2 t_W^2) v_3] \right\}$

TABLE III. Feynman rules of couplings with  $Z$  to charged Higgs and gauge bosons.

The triple couplings of three gauge bosons arise from the covariant kinetic Lagrangian of the non Abelian gauge bosons leading to the involved couplings of  $Z$  given in Table IV.

Vertex	Coupling
$g_{ZW^+ W^-}$	$t_W^{-1} c_\theta$
$g_{ZY^A Y^{-A}}$	$\frac{1}{2s_W} \left[ c_\theta c_W (-1 + \sqrt{3}\beta t_W^2) + s_\theta \sqrt{3 - 3\beta^2 t_W^2} \right]$

TABLE IV. Feynman rules for triple gauge couplings relating with LFV decays.

The remaining couplings of the SM-like Higgs boson and  $Z$  to two Dirac leptons are listed in Table V. It is noted that the couplings of the  $h$  and  $Z$  to two Majorana fermions must be

Vertex	Coupling
$h\bar{e}_a e_a$	$-\frac{im_a}{v} \times \frac{c_\zeta}{c_\beta}$
$Z\bar{e}_a e_a$	$\frac{iec_\theta}{2c_W s_W} \left[ \left( -1 + 2s_W^2 + \frac{t_\theta}{c_W \sqrt{1-\beta^2 t_W^2}} \left( \frac{c_W^2}{\sqrt{3}} - \beta s_W^2 \right) \right) P_L + 2 \left( s_W^2 - \frac{\beta s_W^2 t_\theta}{c_W \sqrt{1-\beta^2 t_W^2}} \right) P_R \right]$
$Z\bar{E}_a E_a$	$\frac{igc_\theta}{2c_W} \left[ \left( (1 - \sqrt{3}\beta)s_W^2 + \frac{3\beta(-1+\sqrt{3}\beta)s_W^2 t_\theta + (-2\sqrt{3}c_W^2)t_\theta}{3c_W \sqrt{1-\beta^2 t_W^2}} \right) + \left( \frac{(-2\sqrt{3}c_W^2)t_\theta}{3c_W \sqrt{1-\beta^2 t_W^2}} \right) P_L \right]$

TABLE V. Feynman rules of couplings with  $Z/h$  to charged leptons.

symmetric for the right expressions for Feynman rules in notations of the four-components Dirac spinor [109]. This is the case of neutrinos with masses generated following the seesaw

mechanism. The Feynman rules now for couplings of a neutral bosons  $Z$  (or  $h$ ) to two Majorana fermions are presented in Fig. VI, corresponding to the following Lagrangian

Vertex	Coupling
$h\bar{n}_i n_j$	$-\frac{ig}{2m_W} (\lambda_{ij}^h P_L + \lambda_{ij}^{h*} P_R)$
$Z_\mu \bar{n}_i n_j$	$ie\gamma^\mu (G_{ij} P_L - G_{ji} P_R)$

TABLE VI. Feynman rules of couplings with  $Z/h$  to two Majorana leptons  $n_i$  and  $n_j$ .

$$\mathcal{L}_{\text{int}} = \sum_{i,j=1}^{3+2K} \left[ -\frac{g}{4m_W} \bar{n}_i (\lambda_{ij}^h P_L + \lambda_{ij}^{h*} P_R) n_j h + \frac{e}{2} \bar{n}_i \gamma^\mu (G_{ij} P_L - G_{ji} P_R) n_j Z_\mu \right], \quad (39)$$

where

$$\lambda_{ij}^h = \lambda_{ji}^h = -\frac{s_\zeta}{s_\beta} \sum_{c=1}^3 (U_{ci}^{\nu*} m_{n_i} U_{cj}^\nu + U_{cj}^{\nu*} m_{n_j} U_{ci}^\nu), \quad (40)$$

$$G_{ij} = \frac{c_\theta}{2c_W s_W} \left[ 1 + \frac{t_\theta}{c_W \sqrt{1 - \beta^2 t_W^2}} \left( \frac{c_W^2}{\sqrt{3}} - \beta s_W^2 \right) \right] q_{ij}, \quad q_{ij} \equiv \sum_{c=1}^3 U_{ci}^{\nu*} U_{cj}^\nu. \quad (41)$$

The relation  $\frac{1}{2} \bar{n}_i \gamma^\mu (G_{ij} P_L - G_{ji} P_R) n_j = \bar{n}_i \gamma^\mu G_{ij} P_L n_j$  was used [109]. After deriving the Feynman rules for vertex couplings, the amplitudes will be written in the same technique for both kinds of Dirac and Majorana fermions appearing in the vertices  $Z\bar{n}_i n_j$  and  $Z\bar{E}_a E_a$ , respectively [109].

The one-loop Feynman diagram for decays  $Z \rightarrow e_a^\pm e_b^\mp$  are shown in Fig. 1. We use the formulas of amplitude for the decay  $Z(q) \rightarrow e_b^+(p_2) e_a^-(p_1)$  in Ref. [81]

$$\mathcal{M}_Z = \frac{e}{16\pi^2} \times \bar{u}_a [\not{\epsilon} (\bar{a}_L P_L + \bar{a}_R P_R) + (p_1 \cdot \epsilon) (\bar{b}_L P_L + \bar{b}_R P_R)] v_b, \quad (42)$$

where  $\epsilon^\mu$  is the polarized vector of the gauge boson  $Z$  and  $\bar{b}_{L,R}$ . The LFVZ partial decay width now is

$$\Gamma(Z \rightarrow e_b^+ e_a^-) = \frac{\sqrt{\lambda}}{16\pi m_Z^3} \left| \frac{e}{16\pi^2} \right|^2 \left( \frac{\lambda H_0}{12m_Z^2} + H_1 + \frac{H_2}{3m_Z^2} \right), \quad (43)$$

where

$$\begin{aligned} \lambda &:= m_Z^4 + m_a^4 + m_b^4 - 2(m_Z^2 m_a^2 + m_Z^2 m_b^2 + m_a^2 m_b^2), \\ H_0 &= (m_Z^2 - m_a^2 - m_b^2) (|\bar{b}_L|^2 + |\bar{b}_R|^2) - 4m_a m_b \text{Re} [\bar{b}_L \bar{b}_R^*] \\ &\quad - 4m_a \text{Re} [\bar{a}_R^* \bar{b}_L + \bar{a}_L^* \bar{b}_R] - 4m_b \text{Re} [\bar{a}_L^* \bar{b}_L + \bar{a}_R^* \bar{b}_R], \end{aligned}$$

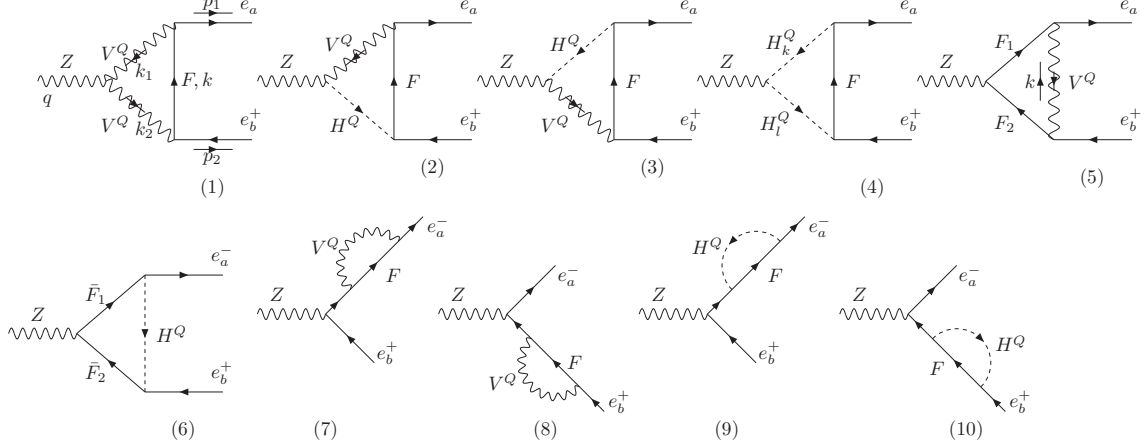


FIG. 1. Feynman diagrams giving one-loop contributions to the decays  $Z \rightarrow e_b^+ e_a^-$  in the unitary gauge, where  $F, F_1, F_2 \equiv n_i, E_a$ ;  $H, H_{k,l} = H^\pm, H^{\pm A}$ ; and  $V = W^\pm, Y^{\pm A}$  in the  $331\beta\text{ISS}(K, K)$  model.

$$\begin{aligned}
 H_1 &= 4m_a m_b \text{Re}(\bar{a}_L \bar{a}_R^*), \\
 H_2 &= \left[ 2m_Z^4 - m_Z^2 (m_a^2 + m_b^2) - (m_a^2 - m_b^2)^2 \right] (|\bar{a}_L|^2 + |\bar{a}_R|^2), \quad (44)
 \end{aligned}$$

where the form factors  $\bar{a}_{L,R}$  arise from loop corrections corresponding to Feynman diagrams shown in Fig. 1. The detailed analytic formulas to  $\bar{a}_{L,R}$  and  $\bar{b}_{L,R}$  are shown in Appendix C based on previous works [81–83]. On the other hand, a new class of one-loop contributions from  $Z$ - $S$ - $V$  diagrams 2 and 3 was computed precisely.

In the unitary gauge, the Feynman diagrams for one-loop contributions to LFVh decays are shown in Fig. 2 [101, 104, 110–112]. The effective Lagrangian of the decays is

$$\mathcal{L}^{\text{LFV}h} = h \bar{e}_a \left[ \Delta_{(ab)L} P_L + \Delta_{(ab)R} P_R \right] e_b + \text{H.c.},$$

where the scalar factors  $\Delta_{(ab)L,R}$  arise from the loop contributions. The partial width is

$$\Gamma(h \rightarrow e_a e_b) \equiv \Gamma(h \rightarrow e_a^- e_b^+) + \Gamma(h \rightarrow e_a^+ e_b^-) \simeq \frac{m_h}{8\pi} (|\Delta_{(ab)L}|^2 + |\Delta_{(ab)R}|^2) \quad (45)$$

with the condition  $m_h^2 \gg m_{a,b}^2$ . Here,  $m_{a,b}$  are the masses of the charged leptons. The on-shell conditions for external particles are  $p_{1,2}^2 = m_{a,b}^2$  and  $q^2 \equiv (p_1 + p_2)^2 = m_h^2$ . The corresponding branching ratio is  $\text{Br}(h \rightarrow e_a e_b) = \Gamma(h \rightarrow e_a e_b) / \Gamma_h^{\text{total}}$ , where  $\Gamma_h^{\text{total}} \simeq 4.1 \times 10^{-3} \text{ GeV}$  [113].

The  $\Delta_{(ab)L,R}$  can be written as

$$\Delta_{(ab)L,R} = \sum_{i=1,5,7,8} \Delta_{(ab)L,R}^{(i)W} + \sum_{i=4,6,9,10} \Delta_{(ab)L,R}^{(i)H}, \quad (46)$$

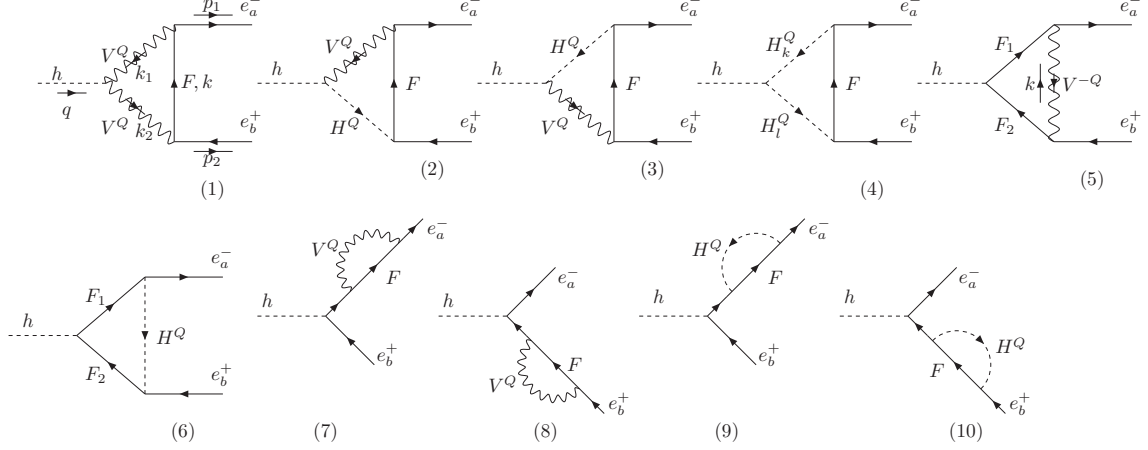


FIG. 2. Feynman diagrams giving one-loop contributions to the decay  $h \rightarrow e_a^- e_b^+$  in the unitary gauge, where  $F, F_1, F_2 \equiv n_i, E_a$ ;  $H, H_{k,l} = H^\pm, H^{\pm A}$ ; and  $V = W^\pm, Y^{\pm A}$ .

where the analytic forms of  $\Delta_{(ab)L,R}^{(i)W}$  and  $\Delta_{(ab)L,R}^{(i)H}$  are shown in Appendix D. We recall here that one-loop contributions from  $E_a, H^{\pm A}$ , and  $Y$  are zeros with assumptions that  $V_{L,R}^E = I_3$  and  $m_{E_a} = m_E \forall a = 1, 2, 3$ .

#### IV. NUMERICAL DISCUSSION

In numerical discussion, we will use the best-fit values of the neutrino oscillation data [114] corresponding to the NO scheme with  $m_{n_1} < m_{n_2} < m_{n_3}$ , namely,

$$s_{12}^2 = 0.32, \quad s_{23}^2 = 0.547, \quad s_{13}^2 = 0.0216, \quad \delta = 218 \text{ [Deg]},$$

$$\Delta m_{21}^2 = 7.55 \times 10^{-5} [\text{eV}^2], \quad \Delta m_{32}^2 = 2.424 \times 10^{-3} [\text{eV}^2]. \quad (47)$$

In numerical calculation, we will use the formulas

$$\hat{m}_\nu = (\hat{m}_\nu^2)^{1/2} = \text{diag} \left( m_{n_1}, \sqrt{m_{n_1}^2 + \Delta m_{21}^2}, \sqrt{m_{n_1}^2 + \Delta m_{21}^2 + \Delta m_{32}^2} \right), \quad (48)$$

$$U_{\text{PMNS}} = \begin{pmatrix} c_{12}c_{13} & c_{13}s_{12} & s_{13}e^{-i\delta} \\ -c_{23}s_{12} - c_{12}s_{13}s_{23}e^{i\delta} & c_{13}c_{23} - s_{12}s_{13}s_{23}e^{i\delta} & c_{13}s_{23} \\ s_{12}s_{23} - c_{12}c_{23}s_{13}e^{i\delta} & -c_{23}s_{12}e^{i\delta}s_{13} - c_{13}s_{23} & c_{13}c_{23} \end{pmatrix}. \quad (49)$$

Similarly for the IO scheme with  $m_{n_3} < m_{n_1} < m_{n_2}$ , we choose experimental data as follows [114]:

$$s_{12}^2 = 0.318_{-0.016}^{+0.016}, \quad s_{23}^2 = 0.578_{-0.010}^{+0.017}, \quad s_{13}^2 = 2.225_{-0.070}^{+0.064} \times 10^{-2}, \quad \delta = 284_{-28}^{+26} \text{ [Deg]},$$

$$\Delta m_{21}^2 = 7.5_{-0.20}^{+0.22} \times 10^{-5} [\text{eV}^2], \quad \Delta m_{32}^2 = -2.52_{-0.02}^{+0.03} \times 10^{-3} [\text{eV}^2]. \quad (50)$$

The active mixing matrix and neutrino masses are determined as

$$\hat{m}_\nu = (\hat{m}_\nu^2)^{1/2} = \text{diag} \left( \sqrt{m_{n_3}^2 - \Delta m_{32}^2 - \Delta m_{21}^2}, \sqrt{m_{n_3}^2 - \Delta m_{32}^2}, m_{n_3} \right). \quad (51)$$

These neutrino masses satisfy automatically the constraint from Plank 2018 [115] that  $\sum_{i=1}^3 m_{n_i} \leq 0.12$  eV. This condition is automatically satisfied in the mISS framework,  $m_{n_1} = 0$  ( $m_{n_3} = 0$ ) for the NO (IO) scheme. In general, the upper bound of the lightest active neutrino mass is  $m_{n_1}(m_{n_3}) < 0.031$  eV in the NO (IO) scheme.

The other well-known numerical parameters are given in Ref. [114], namely,

$$\begin{aligned} g &= 0.652, \quad G_F = 1.166 \times 10^{-5} \text{ GeV}^{-2}, \quad \alpha_e = \frac{1}{137} = \frac{e^2}{4\pi}, \quad s_W^2 = 0.231, \\ m_W &= 80.377 \text{ GeV}, \quad m_Z = 91.1876 \text{ GeV}, \quad m_h = 125.25 \text{ GeV}, \quad \Gamma_Z = 2.4955 \text{ GeV}, \\ m_e &= 5 \times 10^{-4} \text{ GeV}, \quad m_\mu = 0.105 \text{ GeV}, \quad m_\tau = 1.776 \text{ GeV}. \end{aligned} \quad (52)$$

The general  $331\beta$  model predicts a  $SU(3)_L$  scale  $v_3$  indicated to be as large as the order of  $\mathcal{O}(10)$  TeV [9, 13, 96–99]. Therefore, we will fix  $v_3 = 20$  TeV, leading to the suppressed  $Z-Z'$  mixing angle  $\theta \simeq 0$ . For simplicity, we fix  $\theta = 0$ ; therefore all parts relating to  $\beta$  appearing in the coupling factors vanish. Recall that one-loop contributions from  $SU(3)_L$  charged Higgs  $H^A$  and gauge bosons  $Y$  with  $m_Y > 1$  TeV and  $m_{E\mathcal{C}\beta} > 5$  GeV result in the largest values of  $\Delta a_\mu(H^A) \leq \mathcal{O}(10^{-11})$  [14]. These bosons also give zero one-loop contributions to LFV decay amplitudes in the case of  $V_{L,R}^E = I_3$ ; hence they do not play significant roles in our work.

The nonunitary part  $\eta \equiv \frac{1}{2} |R_0 R_0^\dagger| \propto x_0$  of the active neutrino mixing matrix is constrained from studies on electroweak precision, cLFV decays [116–118]. We will choose the values that  $x_0 = |\eta_{33}| \leq 10^{-4}$  in our numerical discussion, consistent with Refs. [119–121].

It was shown that heavy charged Higgs bosons still allow small  $t_\beta$  [9, 96, 122, 123], which supports the  $(g-2)_{e_a}$  data in the models under consideration. The heavy neutrino masses must satisfy the experimental searches [124–127]. Therefore, we scan the following regions of the parameter space:

$$\begin{aligned} t_\beta &\in [0.5, 20]; \quad \alpha \in [0, 2\pi]; \quad x_0 \in [10^{-6}, 10^{-4}]; \quad M_I \in [1, 20] \text{ (TeV)}; \quad m_{H_{1,2}^\pm} \in [1, 5] \text{ (TeV)}; \\ \max [ |Y_{Ia}^h| ], \quad \max [ |Y_{Ia}^\nu| ] &< \sqrt{4\pi} \quad \forall I = 1, 2, \dots, K; \quad a = 1, 2, 3. \end{aligned} \quad (53)$$

We also fix  $\zeta = -\theta_{21}$  corresponding to  $\delta = 0$  to get the SM prediction for Higgs decays consistent with experiments. For investigating the LFVh decay, we apply allowed conditions of Higgs self-couplings discussed in Refs. [9, 128, 129] summarized in Appendix A.

First, we consider the 331mISS model with  $K = 2$ . Before showing the precisely numerical results, we estimate the effects of constraints of  $\text{Br}(e_b \rightarrow e_a \gamma)$  on  $\Delta a_{\mu,e}$  using Eq. (33), with well-known experimental data of  $\Delta a_{e,\mu}$ . Fixing  $c_{(12)R,0}(H^\pm) = c_{(21)R,0}(H^\pm) = 0$  to keep small  $\text{Br}(\mu \rightarrow e \gamma)$ , there are strict relations between  $\Delta a_{e,\mu}$  and  $\text{Br}(e_b \rightarrow e_a \gamma)$  independent with all entries of  $Y^h$ . Namely, the NO scheme predicts that

$$\begin{aligned} \left| \frac{c_{(22)R,0}(H^\pm)}{c_{(32)R,0}(H^\pm)} \right| (\text{NO}) &= \left| \frac{(U_{\text{PMNS}})_{13}(U_{\text{PMNS}})_{22} - (U_{\text{PMNS}})_{12}(U_{\text{PMNS}})_{23}}{(U_{\text{PMNS}})_{22}(U_{\text{PMNS}})_{33} - (U_{\text{PMNS}})_{23}(U_{\text{PMNS}})_{32}} \right| \simeq 1.8, \\ \left| \frac{c_{(11)R,0}(H^\pm)}{c_{(31)R,0}(H^\pm)} \right| (\text{NO}) &= \left| \frac{(U_{\text{PMNS}})_{13}(U_{\text{PMNS}})_{22} - (U_{\text{PMNS}})_{12}(U_{\text{PMNS}})_{23}}{(U_{\text{PMNS}})_{13}(U_{\text{PMNS}})_{32} - (U_{\text{PMNS}})_{12}(U_{\text{PMNS}})_{33}} \right| \simeq 0.62, \end{aligned} \quad (54)$$

where the numerical values corresponding to the best-fit point of  $U_{\text{PMNS}}$  are given in Eq. (49). The experimental constraints of  $\text{Br}(e_b \rightarrow e_a \gamma)$  and  $(g-2)_{e_a}$  are given in Table VII for

$\Delta a_\mu$ :	$ c_{(22)R}  \in [1.44, 2.14] \times 10^{-9} \text{ GeV}^{-1}$
$\Delta a_e$ :	$ c_{(11)R}  \in [1.73, 7.57] \times 10^{-11} \text{ GeV}^{-1}$
$\text{Br}(\mu \rightarrow e \gamma)$ :	$ c_{(21)R} ,  c_{(12)R}  < 1.27 \times 10^{-12} \text{ GeV}^{-1}$
$\text{Br}(\tau \rightarrow e \gamma)$ :	$ c_{(31)R} ,  c_{(13)R}  < 4.15 \times 10^{-10} \text{ GeV}^{-1}$
$\text{Br}(\tau \rightarrow \mu \gamma)$ :	$ c_{(32)R} ,  c_{(23)R}  < 4.68 \times 10^{-10} \text{ GeV}^{-1}$

TABLE VII. Allowed values of  $c_{(ab)R}$  from experiments

$c_{(ab)R}$ , leading to experimental constraints with the  $1\sigma$  ranges of  $\Delta a_{\mu,e}$  given as follows

$$\left| \frac{c_{(22)R}}{c_{(32)R}} \right| > [3.08, 4.1], \quad \left| \frac{c_{(11)R}}{c_{(31)R}} \right| > 0.06. \quad (55)$$

Two results in Eqs. (54) and (55) predict that the  $\text{Br}(\tau \rightarrow \mu \gamma)$  gives  $\Delta a_\mu(H^\pm) \leq 1.16 \times 10^{-9}$  when  $c_{(32)R,0}(H^\pm)$  is the dominant one-loop contribution; see a numerical illustration in Fig. 3, in which we used the simple example that  $\phi = 0$  and  $M_1 = M_2$ ,  $U_N = I_2$ . As a result, the future constraint of  $\text{Br}(\tau \rightarrow \mu \gamma)$  will result in a smaller  $\Delta a_\mu$  than  $10^{-9}$ . In contrast, the remaining eight decay rates depend weakly on  $\Delta a_\mu$ . In contrast, the  $\Delta a_e$  easily satisfies the  $1\sigma$  range. The allowed points we collected here satisfy all experimental LFV constraints of cLFV, LFVh, and LFVZ decays, and the  $1\sigma$  range of  $\Delta a_e$ , while  $\Delta a_\mu \geq 10^{-10}$ . We checked some different choices of  $M_1 \neq M_2$  and  $c_\phi \neq 1$  to confirm that the general results

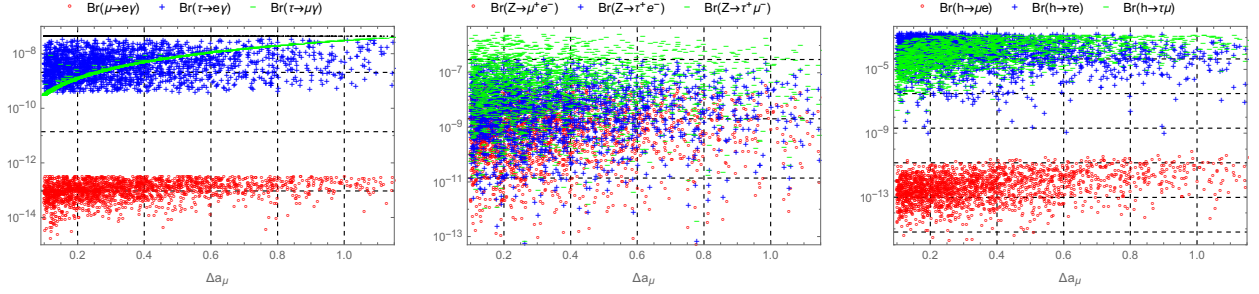


FIG. 3. LFV decay rates as functions of  $\Delta a_\mu$  predicted by the  $331\beta$ mISS model (NO). The black line in the left panel shows the constant value of  $4.2 \times 10^{-8}$ . The narrow green curve in the left panel shows the strict and nearly linear dependence of  $\text{Br}(\tau \rightarrow \mu\gamma)$  on  $\Delta a_\mu$ . The remaining LFV rates do not have this property.

we indicated here in the  $331\beta$ mISS framework are unchanged. In contrast, the LFV decay rates depend weakly on  $\Delta a_e$  in the  $1\sigma$  range of experiments. In addition, all the current and future upper constraints always satisfy the  $(g-2)_e$  data. Therefore, we conclude that the mISS mechanism cannot accommodate the recent  $1\sigma$  data corresponding to  $\Delta a_\mu > 2 \times 10^{-9}$  because of the experimental data of  $\text{Br}(\tau \rightarrow \mu\gamma)$ . Similarly, the IO scheme predicts that

$$\left| \frac{c_{(22)R,0}(H^\pm)}{c_{(32)R,0}(H^\pm)} \right|_{\text{(IO)}} = \left| \frac{(U_{\text{PMNS}})_{12}(U_{\text{PMNS}})_{21} - (U_{\text{PMNS}})_{11}(U_{\text{PMNS}})_{22}}{(U_{\text{PMNS}})_{12}(U_{\text{PMNS}})_{31} - (U_{\text{PMNS}})_{11}(U_{\text{PMNS}})_{32}} \right| \simeq 0.854, \quad (56)$$

implying that  $\Delta a_\mu(H^\pm) \leq 5.5 \times 10^{-10}$ , smaller than the prediction in the NO scheme.

Regarding the  $331\beta$ mISS model ( $K=3$ ), because the qualitative results from the two NO and IO are the same, the numerical discussions will focus on only the NO scheme. The constraints of cLFV decays  $e_b \rightarrow e_a\gamma$  will result in the consequence that dominant contributions from Eq. (34) will be suppressed with  $a \neq b$ . For convenience, all allowed points we collect in the following numerical investigation always satisfy all experimental constraints of LFV decays under consideration as well as the  $1\sigma$  ranges of  $\Delta a_{e,\mu}$ . Consequently, all the figures we depict in the following discussion will also show the allowed ranges of parameters and relevant experimental constraints. For simplicity in numerical investigation, we choose here the simplest case in which  $M_R = M_0 I_3$ , and  $\xi = U_L^e = U_R^e = \hat{\mu}_X = I_3$ , leading to  $\hat{F}_1 = \hat{F}_2 = \hat{F}_3$ . Then, Eq. (33) changes into the following simple form:

$$c_{(ab)R,0}(H^\pm) = \frac{g^2 e v t_\beta^{-1} x_0^{\frac{1}{2}} c_\alpha s_\alpha}{32\sqrt{2}\pi^2 m_W^2} \left( U_{\text{PMNS}} \hat{x}_\nu^{1/2} \hat{\mu}_X^{-1/2} Y^h \right)_{ab} \hat{F}_1. \quad (57)$$

It was shown that the diagonal form of  $c_{(ab)R,0}(H^\pm)$  given in Eq. (33) will result in the allowed range of both  $1\sigma$  experimental data of  $(g-2)_{e,\mu}$  but small LFV decay rates satisfying the current experiments [14]. Therefore, defining the diagonal matrix  $Y^d$ ,

$$(U_{\text{PMNS}}\hat{x}_\nu^{1/2}Y^h)_{ab} = Y_{ab}^d, \quad (58)$$

then we checked that the diagonal form of  $Y_{ab}^d \equiv Y_a^d \delta_{ab}$  can successfully explain that both two  $\Delta a_{e,\mu}$  and LFV decay rates are much smaller than current experimental constraints, except  $\text{Br}(\mu \rightarrow e\gamma)$ . We emphasize that this strict constraint forces  $0 \simeq |Y_{12}^d|, |Y_{21}^d| < 2 \times 10^{-4}$ , which we confirmed by our numerical check. Therefore, choosing to scan arbitrary ranges of  $Y^h$  to collect allowed points satisfying these two relations is much more difficult than scanning all entries of  $Y^d$  fixing  $Y_{12}^d = Y_{21}^d = 0$ . For this reason, we determine the allowed ranges of the parameter space to collect the allowed points mentioned above; the scanning range of  $m_{n_1}$  and  $Y^d$  are chosen as follows:

$$m_{n_1} \in [10^{-4}, 0.032] \text{ eV},$$

$$Y_{22}^d \in [-5, 5], Y_{12}^d = Y_{21}^d = 0, |Y_{ab}^d| \leq 1 \forall (a, b) \neq \{(12), (21), (22)\}. \quad (59)$$

All values of  $m_{n_1}$  and entries of  $Y^d$  will be checked to satisfy the perturbative limits of the Yukawa couplings  $Y^h$  and  $Y^\nu$  generating  $m_D$ . The dependence of LFV decay rates on  $\Delta a_\mu$  is depicted in Fig. 4, showing that all LFV decay rates depend weakly of  $\Delta a_\mu$ . The

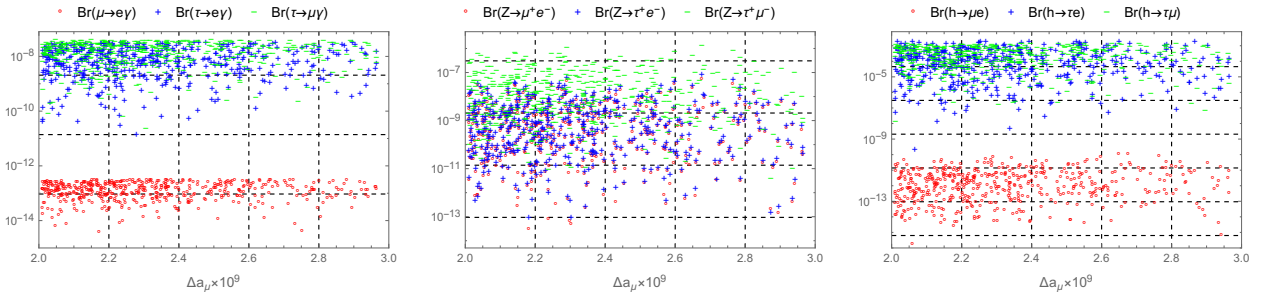


FIG. 4. LFV decay rates as functions of  $\Delta a_\mu$  predicted by the 331 $\beta$ ISS model (NO). All collected points here satisfy all recent LFV decay rates mentioned in this work.

conclusion is the same for  $\Delta a_e$ . Therefore, the  $(g-2)_{\mu,e}$  data cannot predict any significant consequences on LFV decay rates. The upper bounds of  $\text{Br}(e_b \rightarrow e_a \gamma)$ , and  $\text{Br}(h \rightarrow \tau e_a)$  always reach the current experimental constraints, while those of the remaining are:

$$\text{Br}(h \rightarrow \mu e) \leq 10^{-10}, \text{Br}(Z \rightarrow \mu^+ e^-) \leq 5 \times 10^{-8},$$

$$\text{Br}(Z \rightarrow \tau^+ e^-) \leq 8.3 \times 10^{-8}, \quad \text{Br}(Z \rightarrow \tau^+ \mu^-) \leq 1.35 \times 10^{-6}. \quad (60)$$

We can see that the decay channel  $h \rightarrow \mu e$  is invisible for near-future experimental searches. These predictions of  $\text{Br}(h \rightarrow e_b e_a)$  distinguish from other current models allowing large values of  $\max[\text{Br}(h \rightarrow \mu e)] \simeq \mathcal{O}(10^{-5})$  [130]. There are stricter constraints on the parameters than the chosen scanning ranges,  $t_\beta \leq 14$ ,  $0.12 \leq |s_{2\alpha}|$ ,  $10^{-3} < m_{n_1} < 0.03$  eV,  $0.02 < |Y_{11}^d| < 0.2$ ,  $1 < |Y_{22}^d| < 4.5$ ,  $|Y_{31}^d| < 0.35$ , and  $|m_{H_1^\pm} - m_{H_2^\pm}| > 216$  GeV, consistent with the dominant contributions shown in Eq. (33) which must be non-zero to guarantee large  $\Delta a_{e,\mu}$ . This allowed range of small  $t_\beta$  distinguishes with that requiring very large  $t_\beta$  needed in 2HDM models [131]. In addition, the heavy singly charged Higgs masses are allowed, being distinguishable with many 2HDM models [132]. Recall that the numerical results we discuss here use the singly charged Higgs couplings given in Eqs. (31), in which  $c_{(ab)R,0}(H^\pm)$  given in Eq. (33) is not exactly the same. But if  $c_{(ab)R,0}(H^\pm) \propto Y_{ab}^d$  give dominant contributions in  $\Delta a_{e,\mu}$  and LFV decay rates, the following linear relations will appear:  $\Delta a_\mu/\Delta a_e \propto |Y_{22}^d/Y_{11}^d|$  and  $R_{23} \propto R_\gamma, R_Z, R_h$ , where

$$R_{23} \equiv \frac{(Y_{13}^d)^2 + (Y_{31}^d)^2}{(Y_{32}^d)^2 + (Y_{23}^d)^2}, \quad R_\gamma = \frac{\text{Br}(\tau \rightarrow e\gamma)}{\text{Br}(\tau \rightarrow \mu\gamma)}, \quad R_Z = \frac{\text{Br}(Z \rightarrow \tau e)}{\text{Br}(Z \rightarrow \tau\mu)}, \quad R_h = \frac{\text{Br}(h \rightarrow \tau e)}{\text{Br}(h \rightarrow \tau\mu)}.$$

The mentioned relations are illustrated numerically in Fig. 5, confirming that the linear

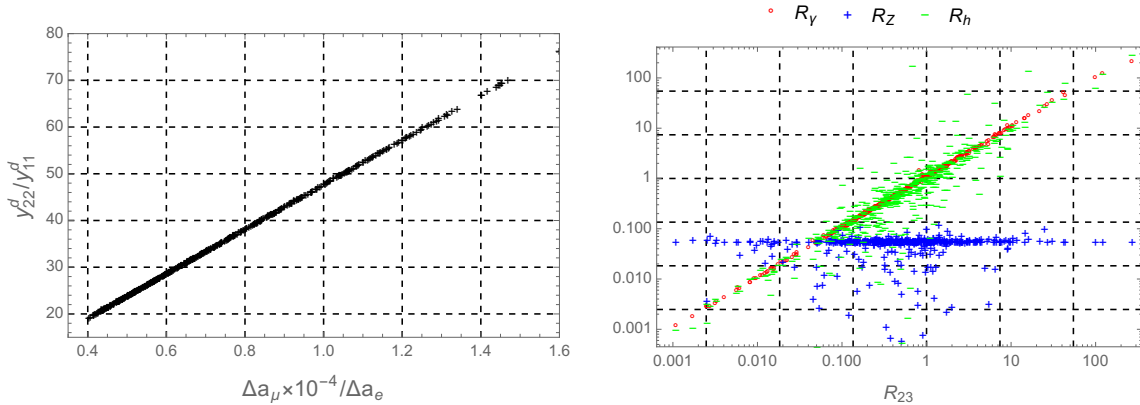


FIG. 5. Linear properties of  $(g-2)_{e,\mu}$  anomalies (LFV decay rates) in the left (right) panel, showing that all  $(g-2)_{\mu,e}$  anomalies and LFV decays rates get dominant one-loop contributions from Yukawa couplings of singly charged Higgs boson, except the LFVZ ones.

relations happen for  $(g-2)_{e,\mu}$  anomalies, cLFV, and LFV $h$  decays, but not for LFVZ one. The reason is that, in the regions of parameters with large LFVZ decay rates, the

amplitudes get dominant one-loop contributions from the  $W$  exchanges, consisting of the part originating from the massive property of the  $Z$ , which does not appear for the photon. The large one-loop contributions from singly charged Higgs result in  $\text{Br}(h \rightarrow \tau e_a)$  being much larger than those predicted by ISS models without Higgs contributions [104, 133–135]. In conclusion, in the  $331\beta$ ISS model, the Yukawa couplings of the singly charged Higgs are sources of dominant one-loop contributions to  $\Delta a_{\mu,e}$ , necessary to explain the  $1\sigma$  deviation between the SM and experimental results. These Yukawa couplings will also be important to explain the future experimental results of cLFV and LFV $h$  signals if they are detected.

We can see more interesting properties of LFV $Z$  decays illustrated in Fig. 6, where

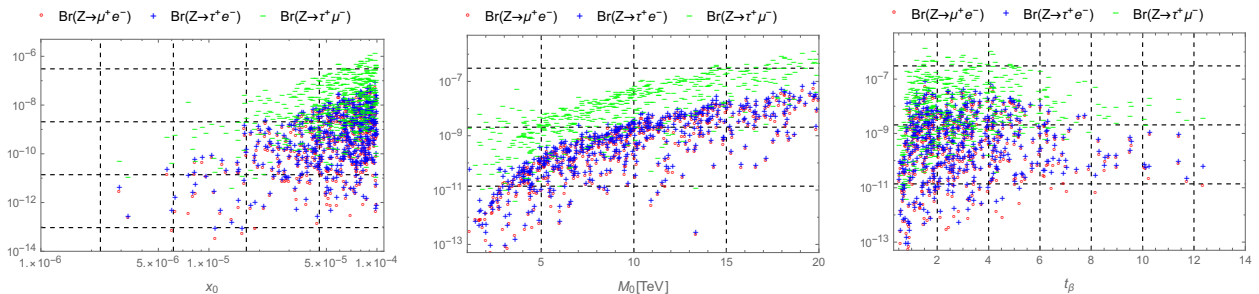


FIG. 6. LFV $Z$  decay rates as functions of  $x_0$ ,  $M_0$ , and  $t_\beta$  in the  $331\beta$ ISS model (NO). The nonunitary factor  $x_0$  strongly affects the maximal values of LFV $Z$  decay rates.

the nonunitary parameter  $x_0$  and heavy ISS neutrino mass scale  $M_0$  significantly affect these decay rates, consistent with ISS models without singly charged Higgs exchanges [83, 84, 86]. The future constraint on  $x_0$  will result in smaller LFV $Z$  decay rates, giving new indirect constraints along with future direct experimental searches for these channels. Large  $\text{Br}(Z \rightarrow e_b^\dagger e_a)$  prefers moderate values of  $t_\beta$  [88], but smaller than those chosen in previous discussion of 2HDM models including supersymmetry [89]. In conclusion, the LFV $Z$  decay rates with ISS neutrinos are significantly larger than those predicted by the 2HDM models with standard seesaw neutrinos [81], including the scotogenic version [136].

As we discussed above for the allowed regions of parameter space,  $t_\beta$  plays an important role similar to that in the 2HDM models. In the  $331\beta$  model, the first two components of Higgs triplets  $\rho$  and  $\eta$  play the same roles discussed in 2HDM [13, 96, 137]. Therefore, the Higgs bosons masses and  $t_\beta$  are also constrained from experiments relating 2HDM models; namely, light  $m_{H_{1,2}^\pm}$  requires large  $t_\beta$ . Also, the popular supersymmetric models inheriting properties of the 2HDM of type II require large  $t_\beta$  to get  $\max[\Delta a_\mu] = 10^{-9}$  [138, 139]. In

contrast, the 331 $\beta$ ISS model predicts that small  $t_\beta$  are supported to get large  $\Delta a_{e,\mu}$  as well as small  $x_0$  consistent with the non-unitary constraints of the active neutrino mixing matrix consistent with future experiments. Figure 7 shows the dependence of free parameters on  $t_\beta$ , pointing out that small  $t_\beta$  allows small  $x_0$  and heavy  $m_{H_{1,2}^\pm}$ . Namely, the large values of  $t_\beta$  in

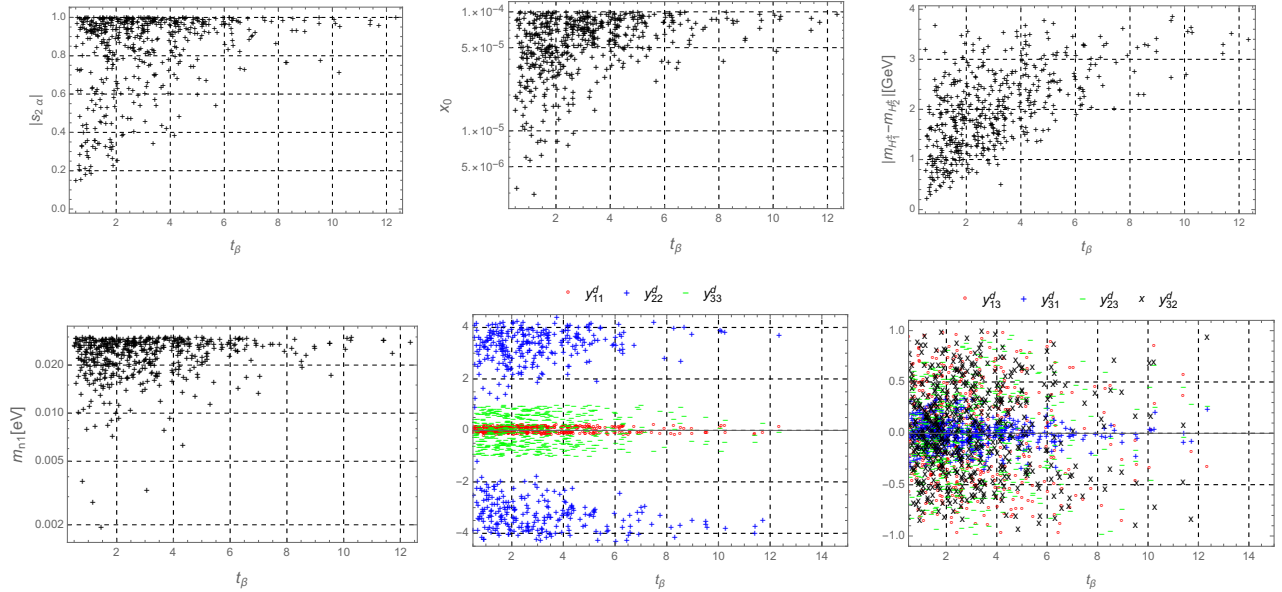


FIG. 7. Parameters of the 331 $\beta$ ISS model as functions of  $t_\beta$ .

the allowed regions require large values of many parameters such as  $|s_{2\alpha}|$ ,  $x_0$ ,  $|m_{H_1^\pm} - m_{H_2^\pm}|$ ,  $m_{n_1}$ , and  $Y_{22}^d$ , so that the  $1\sigma$  allowed ranges of  $\Delta a_{\mu,e}$ . On the other hand, small  $Y_{ab}^d$  with  $a \neq b$  are allowed because they result in small cLFV and LFV $h$  decay rates.

The allowed regions of parameters shown in Fig. 7 may affect the new physics signals at LHC relating to singly charged Higgs bosons. Namely, the non-zero couplings  $H_k^\pm n_a e_a^\mp$  given in Eq. (31) may be large, leading to promising signals of decays  $H_k^\pm \rightarrow e_a^\pm n_a$  searched at LHC such as  $H^\pm \rightarrow \tau^\pm \nu_\tau$  [163]. Consequently, a lower bound of  $m_{H_k^\pm} \geq 500$  GeV is needed. The different values of  $t_\beta$  also affect the singly charged Higgs couplings with quarks similarly to the 2HDM predictions, because the couplings  $H_{1,2}^\pm \bar{t}b \propto \frac{m_t}{vt_\beta} \times \{c_\alpha, s_\alpha\}$  and  $H_{1,2}^\pm \bar{u}d, H_{1,2}^\pm \bar{c}s \propto \frac{m_{u,c} t_\beta}{v} \times \{c_\alpha, s_\alpha\}$  relating to the experimental searches at LHC, excluding large  $t_\beta > 34$  and  $m_{H_k^\pm} > 790$  GeV for  $H^+ \rightarrow \bar{t}b$  [164]. In general, the allowed regions with small  $t_\beta$  and large  $m_{H_k^\pm}$  shown in Fig. 7 are still favored by LHC searches. Apart from that, the Yukawa couplings  $Y_{ab}^h$  affect significantly the couplings of charged Higgs with heavy neutrinos, implying that the decays  $H^\pm \rightarrow e_a^\pm n_i$  may appear at LHC [165–167]. In conclusion, the allowed ranges shown in Fig. 7 will be useful for further studies of these

signatures at LHC.

Finally, we pay attention to the behavior of cLFV and LFV $h$  decay rates on  $t_\beta$  corresponding to some interesting limits of  $Y^d$ . This may help to understand the properties of LFV decays and the consistency with the new physics at LHC we discussed above. Illustrations are depicted in Fig. 8. Because of very strict experimental constraints on  $\text{Br}(\mu \rightarrow e\gamma)$ ,

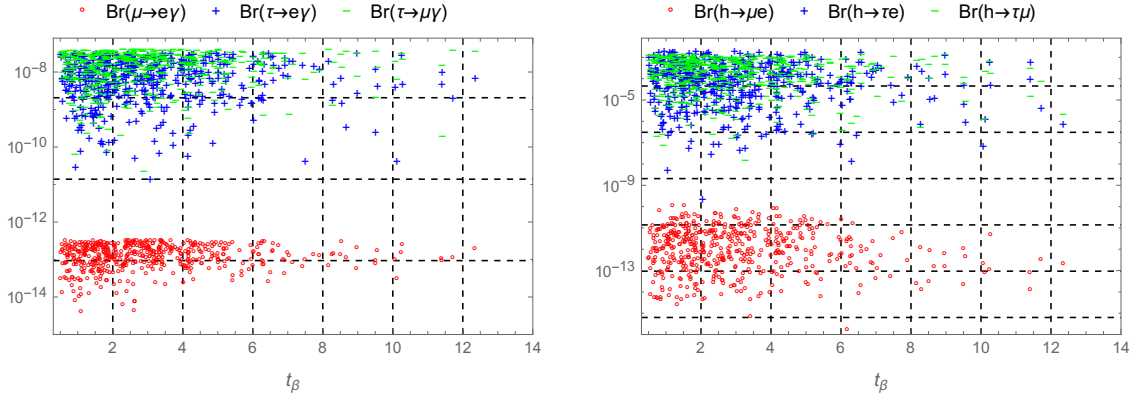


FIG. 8. LFV decay rates as functions of  $t_\beta$  in the  $331\beta$ ISS model (NO) with  $Y_{12}^d = Y_{21}^d = 0$ , while all remaining entries of  $Y^d$  are non-zeros. Large  $t_\beta$  supports only large values of  $\text{Br}(\mu \rightarrow e\gamma)$ ,  $\text{Br}(\tau \rightarrow \mu\gamma)$ , and  $\text{Br}(h \rightarrow \tau\mu)$ .

the condition  $Y_{12}^d = Y_{21}^d = 0$  is necessary, leading to a property shown in the left panel of Fig. 8 that large  $t_\beta$  results in large enough  $\text{Br}(\mu \rightarrow e\gamma)$  to reach the current experimental bound. This also gives a consequence of suppressed  $\text{Br}(h \rightarrow \mu e)$ . We note here that large values of  $\text{Br}(h \rightarrow \tau e, \tau\mu)$  up to the incoming experimental are allowed with small  $t_\beta$  [140]. This property distinguishes 2HDM models supporting large  $t_\beta$  [141] or scotogenic models [136, 142], even without discussion of the experimental  $(g-2)_{e,\mu}$  data [144–147]. The  $331\beta$ ISS model predicts only large  $\text{Br}(\mu \rightarrow e\gamma)$ ,  $\text{Br}(\tau \rightarrow \mu\gamma)$ , and  $\text{Br}(h \rightarrow \tau\mu)$ , and hence the future experimental constraints will give more useful information about  $t_\beta$ .

Let us discuss on the dependence of LFV decay rates on  $t_\beta$  with  $Y_{ab}^d \neq 0$  for  $(a \neq b) = \{(12), (21)\}$ , while other nondiagonal entries of  $Y^d$  vanish, namely  $Y_{23}^d = Y_{32}^d = Y_{13}^d = Y_{31}^d = 0$ . The illustrations are shown in Fig. 9, implying that all chiral enhancement contributions relating to Yukawa couplings of singly charged Higgs boson to all LFV decays vanish. We can see that five decay rates including two cLFV  $\text{Br}(\tau \rightarrow e\gamma, \mu\gamma)$  and three LFV $h$  ones are invisible for incoming experimental sensitivities, while all LFV $Z$  decays behave the same as

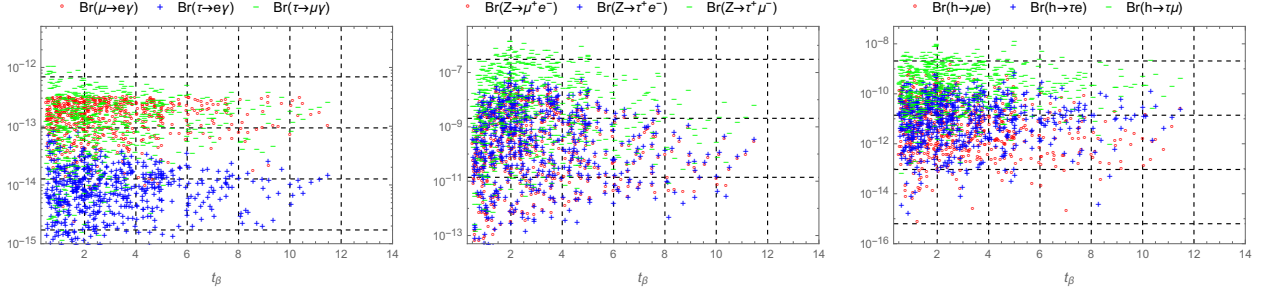


FIG. 9. LFV rates vs.  $t_\beta$  in the  $331\beta\text{ISS}$  model (NO) with non-zeros  $Y_{11}^d, Y_{22}^d, Y_{33}^d, Y_{12}^d, Y_{21}^d \neq 0$ , while  $Y_{13}^d = Y_{31}^d = Y_{23}^d = Y_{32}^d = 0$ .

in the cases of  $Y_{ab}^d \neq 0$ , namely,

$$\text{Br}(\tau \rightarrow e\gamma, \mu\gamma) \leq \mathcal{O}(10^{-12}), \quad \text{Br}(h \rightarrow e_b e_a) \leq \mathcal{O}(10^{-8}).$$

Anyway, the above decay rates are much larger than all results indicated in the 2HDM with standard seesaw neutrinos [81, 136, 141–143]. In conclusion, the results shown in Fig. 9 indicate that any signals of  $\text{Br}(\tau \rightarrow e\gamma, \mu\gamma)$  or  $\text{Br}(h \rightarrow \tau\mu, \tau e)$ , if observed by incoming experiments, will originate from the respective nondiagonal entries of  $Y^d$  shown in the right-hand side of Fig. 5.

## V. CONCLUSIONS

This work discussed the possibilities for the existence of allowed regions of parameters in two frameworks of  $331\beta\text{mISS}$  and  $331\beta\text{ISS}$  models accommodating  $1\sigma$  experimental ranges of  $(g-2)_{e,\mu}$  anomalies and all experimental constraints of LFV decays  $e_a \rightarrow e_a\gamma$ , and  $h, Z \rightarrow e_b^\pm e_a^\mp$ . Dominant one-loop contributions to  $\Delta a_{e_a}$  and decay amplitudes of cLFV and LFVh appearing in the well-known chiral enhancement parts result in precisely the  $331\beta\text{mISS}$  model predicting a strict relation between  $\Delta a_\mu$  and  $\text{Br}(\tau \rightarrow \mu\gamma)$  because of the strict experimental constraint on  $\text{Br}(\mu \rightarrow e\gamma)$ . This leads to the upper bound  $\Delta a_\mu \leq 1.16 \times 10^{-9}$  with  $\text{Br}(\tau \rightarrow \mu\gamma) < 4.2 \times 10^{-8}$ . The  $331\beta\text{ISS}$  is a more interesting model to accommodate  $1\sigma$  data of  $\Delta a_{e,\mu}$  and satisfies all LFV experimental constraints mentioned in this work. The numerical results and qualitative estimations showed that the allowed regions of parameters successfully explaining the  $\Delta a_{\mu,e}$  data support the small  $t_\beta < 15$ , heavy singly charged Higgs boson masses at  $\mathcal{O}(1)$  TeV scale, and small nonunitary scale

$x_0 = \mathcal{O}(10^{-6})$ , which will easily satisfy the future experimental constraints. In addition, we derived qualitative relations that  $\Delta a_{\mu,e} \propto |Y_{11,22}^d|$  and  $\text{Br}(\tau \rightarrow e_a \gamma), \text{Br}(h \rightarrow \tau e_a) \propto (|Y_{3a}^d|^2 + Y_{a3}^d|^2)$  with  $e_a = \mu, e$  and  $a \neq 3$ ; therefore  $\Delta a_{e_a}$  and LFV decay rates depend weakly on each other, except LFVZ ones. Finally, the allowed regions with small  $t_\beta$  predicted by the two models under consideration still predict large LFV $h$  and LFVZ decay rates, reaching incoming experimental sensitivities, except the suppressed  $\text{Br}(h \rightarrow \mu e) < 10^{-10}$ . The allowed regions with small values of  $t_\beta$  and heavy singly charged Higgs bosons will be distinguished from those indicated in available models, in which large  $t_\beta$  is a necessary condition supporting large  $\Delta a_{\mu,e}$  and/or LFV decay rates enough to be detected by incoming experiments.

## ACKNOWLEDGMENTS

We thank Doctor Arindam Das, Doctor Xabier Marcano Imaz, and Dr. Gerardo Hernandez Tome for their discussions. This research is funded by Vietnam National University HoChiMinh City (VNU-HCM) under grant number ‘‘C2022-16-06’’.

## Appendix A: Higgs sector

The scalar potential is [14]

$$\begin{aligned}
V_h = & \mu_1^2 \eta^\dagger \eta + \mu_2^2 \rho^\dagger \rho + \mu_3^2 \chi^\dagger \chi + \lambda_1 (\eta^\dagger \eta)^2 + \lambda_2 (\rho^\dagger \rho)^2 + \lambda_3 (\chi^\dagger \chi)^2 \\
& + \lambda_{12} (\eta^\dagger \eta) (\rho^\dagger \rho) + \lambda_{13} (\eta^\dagger \eta) (\chi^\dagger \chi) + \lambda_{23} (\rho^\dagger \rho) (\chi^\dagger \chi) \\
& + \tilde{\lambda}_{12} (\eta^\dagger \rho) (\rho^\dagger \eta) + \tilde{\lambda}_{13} (\eta^\dagger \chi) (\chi^\dagger \eta) + \tilde{\lambda}_{23} (\rho^\dagger \chi) (\chi^\dagger \rho) + \sqrt{2} f (\epsilon_{ijk} \eta^i \rho^j \chi^k + \text{h.c.}) \\
& + \mu_4^2 h^+ h^- + f_h (\rho^\dagger \eta h^+ + \text{h.c.}) + (h^+ h^-) (\lambda_1^h \eta^\dagger \eta + \lambda_2^h \rho^\dagger \rho + \lambda_3^h \chi^\dagger \chi) + \lambda_4^h (h^+ h^-)^2. \quad (\text{A1})
\end{aligned}$$

The neutral components of all Higgs triplets are expanded as follows:

$$\eta^0 = \frac{1}{\sqrt{2}} (v_1 + r_\eta + i a_\eta), \quad \rho^0 = \frac{1}{\sqrt{2}} (v_2 + r_\rho + i a_\rho), \quad \chi^0 = \frac{1}{\sqrt{2}} (v_3 + r_\chi + i a_\chi). \quad (\text{A2})$$

The relations between the mass and flavor eigenstates of singly charged Higgs bosons are

$$\begin{pmatrix} \eta^\pm \\ \rho^\pm \\ h^\pm \end{pmatrix} = \begin{pmatrix} c_\beta & c_\alpha s_\beta & s_\alpha s_\beta \\ -s_\beta & c_\alpha c_\beta & c_\beta s_\alpha \\ 0 & -s_\alpha & c_\alpha \end{pmatrix} \begin{pmatrix} \phi_W^\pm \\ H_1^\pm \\ H_2^\pm \end{pmatrix}, \quad (\text{A3})$$

where  $\phi_W^\pm$  are the Goldstone bosons of  $W^\pm$ ,  $H_{1,2}^\pm$  are two physical states with masses  $m_{H_{1,2}^\pm}$ , and  $\alpha$  is a new mixing parameter. The parameters  $\alpha$ , and  $m_{H_{1,2}^\pm}$  are chosen as free ones, while  $\mu_4$ ,  $f$ , and  $f_h$  are determined as follows:

$$\begin{aligned} f &= -\frac{c_\beta s_\beta \left( 2c_\alpha^2 m_{H_1^\pm}^2 + 2s_\alpha^2 m_{H_2^\pm}^2 - \tilde{\lambda}_{12} v^2 \right)}{2v_3}, \\ \mu_4^2 &= s_\alpha^2 m_{H_1^\pm}^2 + c_\alpha^2 m_{H_2^\pm}^2 - \frac{1}{2} \left( \lambda_1^h s_\beta^2 v^2 + \lambda_2^h c_\beta^2 v^2 + v_3^2 \lambda_3^h \right), \\ f_h &= -\frac{\sqrt{2} c_\alpha s_\alpha (m_{H_1^\pm}^2 - m_{H_2^\pm}^2)}{v}. \end{aligned} \quad (\text{A4})$$

The mixing angles of Higgs boson will be defined through the ratios

$$s_{ab} \equiv \sin \theta_{ab} = \frac{v_a}{\sqrt{v_a^2 + v_b^2}}, \quad c_{ab} = \sqrt{1 - s_{ab}^2}, \quad t_{ab} = \frac{s_{ab}}{c_{ab}}, \quad t_{12} = t_\beta^{-1}. \quad (\text{A5})$$

where  $a \neq b$  and  $a, b = 1, 2, 3$ .

The identification of the SM-like Higgs boson is presented in Ref. [8]. For neutral Higgs bosons, to avoid the tree-level contribution of SM-like Higgs bosons to the flavor-changing neutral currents (FCNCs) in the quark sector, we follow the aligned limit introduced in Ref. [96], namely,

$$f = -\frac{\lambda_{13} v_3}{t_\beta} = -\lambda_{23} t_\beta v_3. \quad (\text{A6})$$

From this, we will choose  $\lambda_{23}$  and  $\lambda_{13}$  as functions of  $f$ , which is given by Eq. (A4). As a result,  $r_3 \equiv h_3^0$  is a physical  $CP$ -even neutral Higgs boson with mass  $m_{h_3^0}^2 = 2\lambda_3 v_3^2 - \frac{f c_\beta s_\beta v^2}{v_3}$ . There are two other neutral  $CP$ -even Higgs  $h_1^0$  and  $h_2^0$ , in which  $h_1^0 \equiv h$  is identified with the SM-like Higgs boson found at LHC. Denote an independent mixing parameter  $\delta$  that defines  $\zeta$  relating two bases of neutral  $CP$ -even Higgs bosons as follows:

$$\zeta \equiv -\theta_{21} + \delta, \quad \tan 2\delta \sim \mathcal{O} \left( \frac{v^2}{v_3^2} \right). \quad (\text{A7})$$

This leads to the following relations:

$$\begin{pmatrix} r_\eta \\ r_\rho \end{pmatrix} = \begin{pmatrix} c_\zeta & s_\zeta \\ -s_\zeta & c_\zeta \end{pmatrix} \begin{pmatrix} h \\ h_2^0 \end{pmatrix}. \quad (\text{A8})$$

Note that  $t_{21} = t_\beta > 0$  and the couplings of the SM-like Higgs boson are the same as those given in the SM when  $\delta = 0$ .

Choose  $\delta$  and  $m_h$  as input free parameters; the Higgs self-couplings are

$$\lambda_2 = \frac{\lambda_1 (c_\beta^4 c_\delta^2 + c_\beta^2 (s_\beta^2 + 2s_\delta^2) - 2c_\beta s_\delta s_\zeta + s_\beta^4 s_\delta^2)}{t_\beta^2 s_\zeta^2}$$

$$\begin{aligned}
& + \frac{m_h^2 (c_\beta^2 (s_\delta^2 - c_\delta^2) - 4c_\beta c_\delta s_\beta s_\delta + s_\beta^2 (c_\delta^2 - s_\delta^2))}{2s_\beta^2 v^2 s_\zeta^2} - \frac{f s_\delta v_3 (s_\delta - 2c_\beta s_\zeta)}{2c_\beta s_\beta^3 s_\zeta^2 v^2}, \\
\lambda_{12} = & \frac{2\lambda_1}{t_\beta t_\zeta} - \frac{m_h^2}{c_\beta s_\beta t_\zeta v^2} - \frac{f s_\delta v_3}{c_\beta^2 s_\beta s_\zeta v^2}.
\end{aligned} \tag{A9}$$

The Higgs self-couplings satisfy all constraints discussed recently to guarantee the vacuum stability of the Higgs potential, the perturbative limits, and the positive squared masses of all Higgs bosons [9, 128, 129]. We note that in the case of absence of the relations in Eq. (A6), the mixing between SM-like Higgs bosons with other heavy neutral Higgs is still suppressed due to large  $v_3 > 5$  TeV enough to cancel the FCNCs in 3-3-1 models [148]. We list here the necessary conditions relating to the involved Higgs couplings:

$$\lambda_1, \lambda_2 > 0; \lambda_{12} + 2\sqrt{\lambda_1 \lambda_2} > 0, \lambda_{12} + \tilde{\lambda}_{12} + 2\sqrt{\lambda_1 \lambda_2} > 0, |\lambda_{ij}| < 4\pi. \tag{A10}$$

For simplicity, we will fix  $\lambda_1^h = \lambda_2^h = 0$  in numerical investigation.

## Appendix B: Master one-loop functions to $(g-2)_{e_a}$ anomalies and decays $e_b \rightarrow e_a \gamma$

The relevant functions for one-loop contributions to cLFV decays and  $(g-2)_{e_a}$  anomalies mentioned in this work are [107]

$$\begin{aligned}
f_\Phi(x) &= 2\tilde{g}_\Phi(x) = \frac{x^2 - 1 - 2x \log x}{4(x-1)^3}, \\
\tilde{f}_\Phi(x) &= \frac{2x^3 + 3x^2 - 6x + 1 - 6x^2 \log x}{24(x-1)^4}, \\
\tilde{f}_V(x) &= \frac{-4x^4 + 49x^3 - 78x^2 + 43x - 10 - 18x^3 \ln x}{24(x-1)^4},
\end{aligned} \tag{B1}$$

which consistent with previous work for 3-3-1 models [12, 108].

## Appendix C: One-loop contribution to $Z \rightarrow e_b^+ e_a^-$

### 1. PV-functions and general analytic formulas

The one-loop contributions here are calculated using the notations of Passarino functions [149, 150] given in Ref. [151], consistent with LoopTools [152]; see a detailed discussion in Ref. [112]. The Passarino-Veltman (PV) functions used in this work are defined as follows:

$B_\mu^{(i)} \equiv B_1^{(i)} \times (-1)^i p_{i\mu}$  with  $i = 1, 2$ ;  $C_\mu \equiv -C_1 p_{1\mu} + C_2 p_{2\mu}$ ; and

$$C_{\mu\nu} \equiv C_{00} g_{\mu\nu} + C_{11} p_{1\mu} p_{1\nu} + C_{22} p_{2\mu} p_{2\nu} - C_{12} (p_{1\mu} p_{2\nu} + p_{2\mu} p_{1\nu}).$$

Particular notations of the PV-functions used in our formulas are:  $B_{0,1}^{(i)} = B_{0,1}(p_i^2; M_0^2, M_i^2)$ ,  $C_{0,1,2} = C_{0,1,2}(p_1^2, q^2, p_2^2; M_0^2, M_1^2, M_2^2)$ , and  $B_0^{(12)}(M_1^2, M_2^2) = B_0(q^2; M_1^2, M_2^2)$ . The LFV decays of  $B = h, Z$  will give  $q^2 = (p_1 + p_2)^2 = m_B^2$ , while the external momenta are always fixed as  $p_1^2 = m_a^2$ ,  $p_2^2 = m_b^2$ . Linear combinations of PV-functions used in this work are

$$\begin{aligned} X_0 &\equiv C_0 + C_1 + C_2, \quad X_1 \equiv C_{11} + C_{12} + C_1, \quad X_2 \equiv C_{12} + C_{22} + C_2, \quad X_3 \equiv C_1 + C_2, \\ X_{012} &\equiv X_0 + X_1 + X_2, \quad X_{ij} = X_i + X_j. \end{aligned} \quad (\text{C1})$$

We summarize here the Lagrangian parts appearing 331 $\beta$  model that give one-loop contributions to all relevant LFV decays. The details are mentioned in Ref. [8].

The couplings of gauge bosons  $G_\mu$  including  $Z$ , photon  $A_\mu$ ,  $W^\pm$ , and  $Y^{\pm Q_A}$  with leptons arise from their covariant kinetic parts

$$\begin{aligned} \mathcal{L}_{\text{kin}}^f &= \sum_{a=1}^3 (\overline{L_{aL}} \gamma^\mu D_\mu L_{aL} + \overline{\nu_{aR}} \gamma^\mu \partial_\mu \nu_{aR} + \overline{e_{aR}} \gamma^\mu D_\mu e_{aR} + \overline{E_{aR}} \gamma^\mu D_\mu E_{aR}) \\ &= \sum_{F_1, F_2} [\overline{F_1} \gamma^\mu e (g_{ZF_{12}}^L P_L + g_{ZF_{12}}^R P_R) F_2 Z_\mu] + \sum_F e Q_F \overline{F} \gamma^\mu F A_\mu \\ &\quad + \sum_{F,a} [g_{aFG}^L \overline{F} \gamma^\mu P_L e_a G_\mu^{+Q_G} + \text{h.c.}] + \dots, \end{aligned} \quad (\text{C2})$$

where new fermions  $F$  and  $F_{1,2}$  run over all relevant leptons appearing in the 331 $\beta$ ISS( $K, K$ ) model and  $Q_F$  is the electric charge of the fermion  $F$ . The electric charge conservation results in  $Q_G = Q_F + 1$ . The first term in the second line of Lagrangian (C2) is valid for only Dirac fermions. The general Feynman rules for vertex and couplings corresponding to the Lagrangian (C2) are listed in the lines 2, 4, and 6 of the Table VIII. The remaining vertices and couplings in this Table are defined in the following.

The Yukawa Lagrangian (9) results in the couplings of Higgs bosons and leptons. The couplings of the SM-like Higgs boson  $h$  and charged Higgs relevant with this work have the following forms:  $\mathcal{L}^Y = -h \overline{F_1} (g_{hF_{12}}^L P_L + g_{hF_{12}}^R P_R) F_2 - \overline{F} (g_{aFH}^R P_R + g_{aFH}^L P_L) e_a H^{+Q} + \text{h.c.}$ . The corresponding Feynman rules are shown in Table VIII. Note that the couplings relating to a SM charged lepton  $e_a$  must be close to those of the SM.

Vertex	Coupling	Vertex	Coupling
$\bar{F}e_a H^{+Q}$	$-i(g_{aFH}^R P_R + g_{aFH}^L P_L)$	$\bar{e}_a F H^{-Q}$	$-i(g_{aFH}^{R*} P_L + g_{aFH}^{L*} P_R)$
$\bar{F}e_a G_\mu^{+Q}$	$ig_{aFG}^L \gamma^\mu P_L$	$\bar{e}_a F G_\mu^{-Q}$	$ig_{aFG}^{L*} \gamma^\mu P_L$
$A^\lambda G^{+Q\mu} G^{-Q\nu}$	$-ieQ\Gamma_{\lambda\mu\nu}(p_0, p_+, p_-)$	$A^\mu H^{+Q} H^{-Q}$	$ieQ(p_+ - p_-)_\mu$
$A^\mu \bar{e}_a e_a$	$-ie\gamma_\mu$	$A^\mu \bar{F} F$	$ieQ_F \gamma_\mu$
$Z^\lambda G^{+Q\mu} G^{-Q\nu}$	$-iegZGG\Gamma_{\lambda\mu\nu}(p_0, p_+, p_-)$	$Z^\mu H_1^{+Q} H_2^{-Q}$	$iegZH_1 H_2(p_+ - p_-)_\mu$
$Z^\mu \bar{e}_a e_a$	$ie\gamma_\mu (g_{Ze}^L P_L + g_{Ze}^R P_R)$	$Z^\mu \bar{F}_1 F_2$	$ie\gamma_\mu (g_{ZF_{12}}^L P_L + g_{ZF_{12}}^R P_R)$
$Z^\mu G^{+Q\nu} H^{-Q}$	$iegZGHg_{\mu\nu}$	$Z^\mu G^{-Q\nu} H^{+Q}$	$ieg_{ZGH}^* g_{\mu\nu}$
$hG^{+Q\mu} G^{-Q\nu}$	$ighGGg_{\mu\nu}$	$hH_1^{+Q} H_2^{-Q}$	$i\lambda_{hH_1 H_2}$
$h\bar{e}_a e_a$	$-i\frac{m_a}{v}\delta_{hee}$	$h\bar{F}_1 F_2$	$-i(g_{hF_{12}}^L P_L + g_{hF_{12}}^R P_R)$
$hH^{+Q} G^{-Q\mu}$	$-ig_{hHG}^*(p_0 - p_+)_\mu$	$hH^{-Q} G^{+Q\mu}$	$ig_{hHG}(p_0 - p_-)_\mu$

TABLE VIII. General Feynman rules for vertices and couplings giving one-loop contributions to LFV decays and  $(g-2)_{e_a}$  anomalies in the 331 $\beta$ ISS( $K, K$ ) model.

The couplings of Higgs and gauge bosons are contained in the covariant kinetic terms of the Higgs bosons

$$\begin{aligned}
\mathcal{L}_{\text{kin}}^S &= \sum_{S=\chi, \rho, \eta} (D_\mu S)^\dagger (D^\mu S) \\
&= \sum_G g_{hGG} g_{\mu\nu} h G^{-Q\mu} G^{Q\nu} \\
&\quad + \sum_{H, G} [-ig_{hHG}^* (H^{+Q} \partial_\mu h - h \partial_\mu H^{+Q}) G^{-Q\mu} + ig_{hHG} (H^{-Q} \partial_\mu h - h \partial_\mu H^{-Q}) G^{Q\mu}] \\
&\quad + \sum_H ieQA^\mu (H^{-Q} \partial_\mu H^Q - H^Q \partial_\mu H^{-Q}) + \sum_{k, l} iegZH_k H_l Z^\mu (H_k^{-Q} \partial_\mu H_l^Q - H_l^{Qk} \partial_\mu H_k^{-Q}) \\
&\quad + \sum_{H, G} Z^\mu e [iegZGH G^{Q\nu} H^{-Q} g_{\mu\nu} + ig_{ZGH}^* G^{-Q\nu} H^Q g_{\mu\nu}] + \dots, \tag{C3}
\end{aligned}$$

where sums are taken over  $H, H_k, H_l = H^\pm, H^{\pm A}, H^{\pm B}$ , and gauge bosons  $G = W, Y, V$ .

The triple couplings of three gauge bosons arise from the covariant kinetic Lagrangian of the non-Abelian gauge bosons

$$\mathcal{L}_D^g = -\frac{1}{4} \sum_{a=1}^8 F_{\mu\nu}^a F^{a\mu\nu}, \tag{C4}$$

where

$$F_{\mu\nu}^a = \partial_\mu W_\nu^a - \partial_\nu W_\mu^a + g \sum_{b,c=1}^8 f^{abc} W_\mu^b W_\nu^c, \quad (\text{C5})$$

where  $f^{abc}$  ( $a, b, c = 1, 2, \dots, 8$ ) are structure constants of the  $SU(3)$  group. Changing into the momentum space using  $\partial_\mu \rightarrow -ip_\mu$ , the relevant couplings are defined as

$$\begin{aligned} \mathcal{L}_D^g \rightarrow & -eg_{ZVV} Z^\mu(p_0) V^{+Q\nu}(p_+) V^{-Q\lambda}(p_-) \times \Gamma_{\mu\nu\lambda}(p_0, p_+, p_-), \\ & -eQA^\mu(p_0) V^{+Q\nu}(p_+) V^{-Q\lambda}(p_-) \times \Gamma_{\mu\nu\lambda}(p_0, p_+, p_-), \end{aligned} \quad (\text{C6})$$

where  $\Gamma_{\mu\nu\lambda}(p_0, p_+, p_-) \equiv g_{\mu\nu}(p_0 - p_+)_\lambda + g_{\nu\lambda}(p_+ - p_-)_\mu + g_{\lambda\mu}(p_- - p_0)_\lambda$ , and  $G = W, V, Y$ . This class of couplings was given in Tables I and IV, for the decays  $e_b \rightarrow e_a \gamma$  and  $Z \rightarrow e_a e_b$ , respectively.

One-loop form factors from diagram 1 of Fig. 1 calculated in the unitary gauge are well known from Refs. [82, 83], but for only  $W$  exchange. Because the similar diagrams with  $V$  exchanges have the same forms of Feynman rules, they can be derived in the same way. The general Feynman rules are listed in Table VIII, where we use the relations

$$\sum_F g_{aFG}^{L*} g_{bFG}^L, \sum_{F_{1,2}} g_{aF_1G}^{L*} g_{bF_2G}^L g_{ZF_{12}}^L, \sum_{F_{1,2}} g_{aF_1G}^{L*} g_{bF_2G}^L g_{ZF_{12}}^R \propto \delta_{ab}$$

for both  $F = E_a, n_i$  in this work. Therefore, we can write the following expressions for both  $W, V \equiv G$ :

$$\begin{aligned} \bar{a}_l^{FGG} = \sum_F g_{ab}^{LL} g_{ZGG} \left\{ \left[ -4 + \frac{m_F^2}{m_G^2} \left( \frac{m_Z^2}{m_G^2} - 2 \right) \right] C_{00} + 2(m_Z^2 - m_a^2 - m_b^2) X_3 \right. \\ \left. - \frac{1}{m_G^2} \left[ m_Z^2 (2m_F^2 C_0 + m_a^2 C_1 + m_b^2 C_2) \right. \right. \\ \left. \left. - m_F^2 (B_0^{(1)} + B_0^{(2)}) - m_a^2 B_1^{(1)} - m_b^2 B_1^{(2)} \right] \right\}, \end{aligned} \quad (\text{C7})$$

$$\bar{a}_r^{FGG} = \sum_F g_{ab}^{LL} g_{ZGG} m_a m_b \left[ \left( -4 + \frac{m_Z^2}{m_G^2} \right) X_3 + \frac{m_Z^2 - 2m_G^2}{m_G^4} C_{00} \right], \quad (\text{C8})$$

$$\bar{b}_l^{FGG} = \sum_F g_{ab}^{LL} g_{ZGG} m_a \left[ 4(X_3 - X_1) + \frac{m_Z^2 - 2m_G^2}{m_G^4} (m_F^2 X_{01} + m_b^2 X_2) - \frac{2m_Z^2}{m_G^2} C_2 \right], \quad (\text{C9})$$

$$\bar{b}_r^{FGG} = \sum_F g_{ab}^{LL} g_{ZGG} m_b \left[ 4(X_3 - X_2) + \frac{m_Z^2 - 2m_G^2}{m_G^4} (m_F^2 X_{02} + m_a^2 X_1) - \frac{2m_Z^2}{m_G^2} C_1 \right], \quad (\text{C10})$$

where  $g_{ab}^{LL} \equiv g_{aFG}^{L*} g_{bFG}^L$ ,  $B_{0,1}^{(k)} = B_{0,1}^{(k)}(p_k^2; m_F^2, m_G^2)$ ,  $C_{k,kl} = C_{k,kl}(m_a^2, m_Z^2, m_b^2; m_F^2, m_G^2, m_G^2)$ , and  $X_{0,k,kl}$  are defined in terms of the PV-functions in Eq. (C1) for all  $k, l = 0, 1, 2$ . For

simplicity, the arguments of PV-functions and their linear combinations are written specifically as  $(m_a^2, m_Z^2, m_b^2; m_F^2, m_G^2, m_G^2)$  or  $(M_0^2, M_1^2, M_2^2) = (m_F^2, m_G^2, m_G^2)$  when  $q^2$  is determined precisely. We will use this simple notations from now on.

One-loop form factors from diagram 5 in Fig. 1 are

$$\begin{aligned} \bar{a}_l^{GFF} = \sum_{F_{1,2}} \frac{g_{ab}^{LL}}{m_G^2} \left\{ g_{ZF_{12}}^L \left[ m_G^2 \left( 4C_{00} + 2m_a^2 X_{01} + 2m_b^2 X_{02} - 2m_Z^2 (C_{12} + X_0) \right) \right. \right. \\ \left. \left. - (m_{F_1}^2 - m_a^2) B_0^{(1)} - (m_{F_2}^2 - m_b^2) B_0^{(2)} + m_a^2 B_1^{(1)} + m_b^2 B_1^{(2)} \right. \right. \\ \left. \left. + (m_{F_2}^2 m_a^2 + m_{F_1}^2 m_b^2 - m_a^2 m_b^2) X_0 - m_{F_1}^2 m_{F_2}^2 C_0 - m_{F_1}^2 m_b^2 C_1 - m_{F_2}^2 m_a^2 C_2 \right] \right. \\ \left. - g_{ZF_{12}}^R m_{F_1} m_{F_2} \left[ 2m_W^2 C_0 - 2C_{00} - m_a^2 C_{11} - m_b^2 C_{22} + (m_Z^2 - m_a^2 - m_b^2) C_{12} \right] \right\}, \end{aligned} \quad (C11)$$

$$\bar{a}_r^{GFF} = \sum_{F_{1,2}} \frac{g_{ab}^{LL} m_a m_b}{m_G^2} g_{ZF_{12}}^L \left[ 2C_{00} + 2m_G^2 X_0 + m_a^2 X_1 + m_b^2 X_2 - m_Z^2 C_{12} - m_{F_1}^2 C_1 - m_{F_2}^2 C_2 \right], \quad (C12)$$

$$\bar{b}_l^{GFF} = \sum_{F_{1,2}} \frac{2m_a}{m_G^2} g_{ab}^{LL} \left[ g_{ZF_{12}}^L (-2m_G^2 X_{01} - m_b^2 X_2 + m_{F_2}^2 C_2) - g_{ZF_{12}}^R m_{F_1} m_{F_2} (X_1 - C_1) \right], \quad (C13)$$

$$\bar{b}_r^{GFF} = \sum_{F_{1,2}} \frac{2m_b}{m_G^2} g_{ab}^{LL} \left[ g_{ZF_{12}}^L (-2m_G^2 X_{02} - m_a^2 X_1 + m_{F_1}^2 C_1) - g_{ZF_{12}}^R m_{F_1} m_{F_2} (X_2 - C_2) \right], \quad (C14)$$

where  $g_{ab}^{LL} \equiv g_{aF_1G}^{L*} g_{bF_2G}^L$ , and arguments for PV-functions are  $(m_G^2, m_{F_1}^2, m_{F_2}^2)$ .

The form factors for sum contributions from two diagrams 7 and 8 in Fig. 1 are

$$\begin{aligned} \bar{a}_l^{FG} = \sum_F \frac{g_{aFG}^{L*} g_{bFG}^L g_{Ze}^L}{m_G^2 (m_a^2 - m_b^2)} \left\{ 2m_F^2 (m_a^2 B_0^{(1)} - m_b^2 B_0^{(2)}) + m_a^4 B_1^{(1)} - m_b^4 B_1^{(2)} \right. \\ \left. + (2m_G^2 + m_F^2) (m_a^2 B_1^{(1)} - m_b^2 B_1^{(2)}) \right\}. \end{aligned} \quad (C15)$$

$$\begin{aligned} \bar{a}_r^{FG} = \sum_F \frac{m_a m_b g_{aFG}^{L*} g_{bFG}^L g_{Ze}^R}{m_G^2 (m_a^2 - m_b^2)} \left\{ 2m_F^2 (B_0^{(1)} - B_0^{(2)}) + m_a^2 B_1^{(1)} - m_b^2 B_1^{(2)} \right. \\ \left. + (2m_G^2 + m_F^2) (B_1^{(1)} - B_1^{(2)}) \right\}, \end{aligned} \quad (C16)$$

$$\bar{b}_l^{FG} = \bar{b}_r^{FG} = 0, \quad (C17)$$

where  $g_{ab}^{LL} \equiv g_{aFG}^{L*} g_{bFG}^L$  and  $B_{0,1}^{(k)} = B_{0,1}^{(k)}(p_k^2; m_F^2, m_G^2)$  with  $k = 1, 2$ .

The two diagrams 2 and 3 appearing in the model under consideration were not discussed

previously; we list here for completeness the form factors of diagram 3

$$\begin{aligned}
\bar{a}_l^{FGH} &= \sum_F -\frac{g_{ZGH}g_{aFG}^{L*}}{m_G^2} \left[ g_{bFH}^L m_F (m_G^2 C_0 - C_{00}) - g_{bFH}^R m_b m_G^2 C_2 \right], \\
\bar{a}_r^{FGH} &= \sum_F -\frac{g_{ZGH}g_{aFG}^{L*}}{m_G^2} \times g_{bFH}^R m_a (C_{00} + m_G^2 C_1), \\
\bar{b}_l^{FGH} &= \sum_F -\frac{g_{ZGH}g_{aFG}^{L*}}{m_G^2} \left[ m_a (g_{bFH}^R m_b X_2 - g_{bFH}^L m_F X_{01}) \right], \\
\bar{b}_r^{FGH} &= \sum_F -\frac{g_{ZGH}g_{aFG}^{L*}}{m_G^2} \left[ g_{bFH}^R (m_F^2 X_0 + m_a^2 X_1 - 2m_G^2 C_1) - g_{bFH}^L m_F m_b X_2 \right], \quad (C18)
\end{aligned}$$

where arguments for PV-funtions are  $(m_F^2, m_G^2, m_H^2)$ .

The form factors relating to diagram 3 are

$$\begin{aligned}
\bar{a}_l^{FHG} &= \sum_F -\frac{g_{ZGH}g_{bFG}^L}{m_G^2} \left[ g_{aFH}^{L*} m_F (m_G^2 C_0 - C_{00}) - g_{aFH}^{R*} m_a m_G^2 C_1 \right], \\
\bar{a}_r^{FHG} &= \sum_F -\frac{g_{ZGH}g_{bFG}^L}{m_G^2} \left[ g_{aFH}^{R*} m_b (m_G^2 C_2 + C_{00}) \right], \\
\bar{b}_l^{FHG} &= \sum_F -\frac{g_{ZGH}g_{bFG}^L}{m_G^2} \left[ g_{aFH}^{R*} (m_F^2 X_0 + m_b^2 X_2 - 2m_G^2 C_2) - g_{aFH}^{L*} m_a m_F X_1 \right], \\
\bar{b}_r^{FHG} &= \sum_F -\frac{g_{ZGH}g_{bFG}^L m_b}{m_G^2} \left[ g_{aFH}^{R*} m_a X_1 - g_{aFH}^{L*} m_F X_{02} \right], \quad (C19)
\end{aligned}$$

where arguments for PV-funtions are  $(m_F^2, m_H^2, m_G^2)$ .

The one-loop contributions from the scalar exchanges are well known previously [81, 82], and we list them here using the general Feynman rules listed in Table VIII. Form factors corresponding to diagrams 4 are

$$\begin{aligned}
\bar{a}_l^{FH_k H_l} &= -\sum_F 2g_{ZH_k H_l} g_{aFH_k}^{L*} g_{bFH_l}^L C_{00}, \\
\bar{a}_r^{FH_k H_l} &= -\sum_F 2g_{ZH_k H_l} g_{aFH}^{R*} g_{bFH}^R C_{00}, \\
\bar{b}_l^{FH_k H_l} &= -\sum_F 2g_{ZH_k H_l} \left[ m_a g_{aFH_k}^{L*} g_{bFH_l}^L X_1 + m_b g_{aFH_k}^{R*} g_{bFH_l}^R X_2 - m_F g_{aFH_k}^{R*} g_{bFH_l}^L X_0 \right], \\
\bar{b}_r^{FH_k H_l} &= -\sum_F 2g_{ZH_k H_l} \left[ m_a g_{aFH_k}^{R*} g_{bFH_l}^R X_1 + m_b g_{aFH_k}^{L*} g_{bFH_l}^L X_2 - m_F g_{aFH_k}^{L*} g_{bFH_l}^R X_0 \right], \quad (C20)
\end{aligned}$$

where arguments for PV-funtions are  $(m_F^2, m_{H_k}^2, m_{H_l}^2)$ .

Forms factors corresponding to diagram 6 are

$$\bar{a}_l^{HFF} = -\sum_{F_1, F_2} \left\{ g_{ZF_{12}}^L \left[ g_{ab}^{LL} m_{F_1} m_{F_2} C_0 + g_{ab}^{RL} m_a m_{F_2} (C_0 + C_1) \right] \right.$$

$$\begin{aligned}
& + g_{ab}^{LR} m_b m_{F_1} (C_0 + C_2) + g_{ab}^{RR} m_a m_b X_0 \Big] \\
& + g_{ZF_{12}}^R \left[ -g_{ab}^{LL} (2C_{00} + m_a^2 X_1 + m_b^2 X_2 - m_Z^2 C_{12}) \right. \\
& \quad \left. - m_a m_{F_1} g^{RL} C_1 - m_b m_{F_2} g^{LR} C_2 \right] \Big\} \\
\bar{a}_r^{HFF} = & - \sum_{F_1, F_2} \left\{ g_{ZF_{12}}^L \left[ -g_{ab}^{RR} (2C_{00} + m_a^2 X_1 + m_b^2 X_2 - m_Z^2 C_{12}) \right. \right. \\
& \quad \left. \left. - g^{LR} m_a m_{F_1} C_1 - g^{RL} m_b m_{F_2} C_2 \right] \right. \\
& + g_{ZF_{12}}^R \left[ g_{ab}^{RR} m_{F_1} m_{F_2} C_0 + g_{ab}^{LR} m_a m_{F_2} (C_0 + C_1) \right. \\
& \quad \left. + g_{ab}^{RL} m_b m_{F_1} (C_0 + C_2) + g_{ab}^{LL} m_a m_b X_0 \right] \Big\}, \\
\bar{b}_l^{HFF} = & - \sum_{F_1, F_2} 2 \left[ g_{ZF_{12}}^L (g_{ab}^{RL} m_{F_2} C_2 + g_{ab}^{RR} m_b X_2) + g_{ZF_{12}}^R (g_{ab}^{RL} m_{F_1} C_1 + g_{ab}^{LL} m_a X_1) \right], \\
\bar{b}_r^{HFF} = & - \sum_{F_1, F_2} 2 \left[ g_{ZF_{12}}^L (g_{ab}^{LR} m_{F_1} C_1 + g_{ab}^{RR} m_a X_1) + g_{ZF_{12}}^R (g_{ab}^{LR} m_{F_2} C_2 + g_{ab}^{LL} m_b X_2) \right], \quad (C21)
\end{aligned}$$

where  $g_{ab}^{XY} \equiv g_{aF_1H}^{X*} g_{bF_2H}^Y$  with  $X, Y = L, R$ , and arguments for PV-funtions are  $(m_H^2, m_{F_1}^2, m_{F_2}^2)$ .

The form factors in Eq. (C21) are also applicable for Majorana fermions, for example

$g_{ZF_{12}}^L \equiv G_{ij}$  and  $g_{ZF_{12}}^R \equiv -G_{ji}$  defined in Eq. (39).

The sum of two diagrams 9 and 10 gives

$$\begin{aligned}
\bar{a}_l^{FH} = & \sum_F -\frac{g_{Ze}^L}{m_a^2 - m_b^2} \left[ m_F (m_a g_{ab}^{RL} + m_b g_{ab}^{LR}) (B_0^{(1)} - B_0^{(2)}) \right. \\
& \quad \left. - m_a m_b g_{ab}^{RR} (B_1^{(1)} - B_1^{(2)}) - g_{ab}^{LL} (m_a^2 B_1^{(1)} - m_b^2 B_1^{(2)}) \right], \\
\bar{a}_r^{FH} = & \sum_F -\frac{g_{Ze}^R}{m_a^2 - m_b^2} \left[ m_F (m_a g_{ab}^{LR} + m_b g_{ab}^{RL}) (B_0^{(1)} - B_0^{(2)}) \right. \\
& \quad \left. - m_a m_b g_{ab}^{LL} (B_1^{(1)} - B_1^{(2)}) - g_{ab}^{RR} (m_a^2 B_1^{(1)} - m_b^2 B_1^{(2)}) \right], \quad (C22)
\end{aligned}$$

where  $g_{ab}^{XY} = g_{aFH}^{X*} g_{bFH}^Y$  with  $X, Y = L, R$ , and  $B_{0,1}^{(k)} = B_{0,1}(p_k^2; m_F^2, m_H^2)$ .

## 2. Particular forms for the 331 $\beta$ ISS( $K, K$ ) model

From the general analytical formulas listed in Eq. (C7) to Eq. (C22), the two particular contributions in our work that  $G = W, V$ , we compute them based on the following replacements. In particular, for  $G = W$  exchange and  $F = n_i$ , we compute them based on the replacements

$$\{F, F_1, F_2, G\} = \{n_i, n_i, n_j, W\}, \quad (C23)$$

and the general vertex factors given in Table VIII are matched to the Feynman rules of  $W^\pm$ , namely,

$$\{g_{aFG}^L, g_{ZGG}, g_{ZF_{12}}^L, g_{ZF_{12}}^R\} = \left\{ \frac{g}{\sqrt{2}}(U_0^{\nu\dagger}U_L^\epsilon)_{ia}, g_{ZW^+W^-}, G_{ij}, -G_{ji} \right\}, \quad (\text{C24})$$

which are shown in Tables I and II; and Eq. (40). The formulas of  $g_{Ze}^{L(R)}$  are shown in the second line of Table V, consistent with the SM results in the limit  $\theta = 0$ , namely,

$$g_{ZW^+W^-} = t_W^{-1}, \quad g_{Zee}^L = \frac{-1 + 2s_W^2}{2c_W s_W}, \quad g_{Zee}^R = t_W.$$

Similarly, the one-loop contributions of  $G = V$  exchange and  $F = E_a$  are computed easily.

#### Appendix D: One-loop contributions to $h \rightarrow e_b e_a$ in the 331ISS( $K, K$ ) model

First, we will present here general form factors for all one-loop contributions. The one-loop contributions of a gauge boson  $G$  corresponding to diagrams 1 and the sum of two diagrams 7 and 8 in Fig. 2 are

$$\begin{aligned} \Delta_L^{FGG} &= -\frac{1}{16\pi^2} \sum_F g_{ab}^{LL} g_{hGG} \left\{ -m_F^2 \left( B_0^{(1)} + B_0^{(2)} + B_1^{(1)} \right) - m_b^2 B_1^{(2)} + (2m_G^2 + m_h^2) m_F^2 C_0 \right. \\ &\quad \left. + [m_F^2 (2m_G^2 + m_h^2) + 2m_G^2 (2m_G^2 + m_a^2 - m_b^2)] C_1 \right. \\ &\quad \left. + [2m_G^2 (m_a^2 - m_h^2) + m_b^2 m_h^2] C_2 \right\}, \\ \Delta_R^{FGG} &= -\frac{1}{16\pi^2} \sum_F g_{ab}^{LL} g_{hGG} \left\{ -m_F^2 \left( B_0^{(1)} + B_0^{(2)} + B_1^{(2)} \right) - m_a^2 B_1^{(1)} + (2m_G^2 + m_h^2) m_F^2 C_0 \right. \\ &\quad \left. + [m_F^2 (2m_G^2 + m_h^2) + 2m_G^2 (2m_G^2 - m_a^2 + m_b^2)] C_2 \right. \\ &\quad \left. + [2m_G^2 (m_b^2 - m_h^2) + m_a^2 m_h^2] C_1 \right\}, \\ \Delta_L^{FG} &= \sum_F \frac{g\delta_{hee} g^{LL} m_a m_b^2}{(32\pi^2) m_W m_G^2 (m_a^2 - m_b^2)} \\ &\quad \times \left[ 2m_F^2 \left( B_0^{(2)} - B_0^{(1)} \right) + (2m_G^2 + m_F^2) \left( B_1^{(2)} - B_1^{(1)} \right) + m_b^2 B_1^{(2)} - m_a^2 B_1^{(1)} \right], \\ \Delta_R^{FG} &= \frac{m_a}{m_b} \Delta_L^{FG}, \end{aligned} \quad (\text{D1})$$

where  $g^{LL} \equiv g_{aFG}^{L*} g_{bFG}^L$ , and arguments for PV-funtions are  $(m_a^2, m_h^2, m_b^2; m_F^2, m_G^2, m_G^2)$ .

Diagrams 5 in Fig. 2:

$$\Delta_L^{GFF} = \sum_{F_1, F_2} \frac{m_a g^{LL}}{16\pi^2 m_G^2} \left\{ g_{hF_{12}}^L m_{F_1} \left[ \left( B_1^{(1)} + (2m_G^2 + m_{F_2}^2 - m_b^2) \right) C_1 \right] \right\}$$

$$\Delta_R^{GFF} = \sum_{F_1, F_2} \frac{m_b g^{LL}}{16\pi^2 m_G^2} \left\{ g_{hF_{12}}^L m_{F_1} \left[ -B_0^{(12)} + m_G^2 C_0 + (2m_G^2 + m_{F_1}^2 - m_a^2) C_1 \right] \right. \\ \left. + g_{hF_{12}}^R m_{F_2} \left[ -B_0^{(12)} + m_G^2 C_0 + (2m_G^2 + m_{F_1}^2 - m_a^2) C_1 \right] \right\}, \\ \left\{ g_{hF_{12}}^L m_{F_1} \left[ -B_0^{(12)} + m_G^2 C_0 + (2m_G^2 + m_{F_2}^2 - m_b^2) C_2 \right] \right. \\ \left. + g_{hF_{12}}^R m_{F_2} \left[ (B_1^{(2)} + (2m_G^2 + m_{F_1}^2 - m_a^2)) C_2 \right] \right\},$$

where  $g^{LL} \equiv g_{aF_1G}^{L*} g_{bF_2G}^L$ , and arguments for PV-funtions are  $(m_G^2, m_{F_1}^2, m_{F_2}^2)$ .

The one-loop contributions from scalar exchange in diagrams 4, 6, and the sum of the two diagrams 9 and 10 are denoted as  $\Delta_{L(R)}^{FH_1H_2}$ ,  $\Delta_{L(R)}^{HF_1F_2}$ , and  $\Delta_{L(R)}^{FH}$ . The particular formulas of  $\Delta_{L(R)}^{FH_1H_2}$  and  $\Delta_{L(R)}^{FH}$  are

$$\Delta_L^{FH_1H_2} = \frac{\lambda_{hH_1H_2}}{16\pi^2} \sum_F \left[ g^{RL} m_F C_0 - g^{LL} m_a C_1 - g^{RR} m_b C_2 \right], \quad (D2)$$

$$\Delta_R^{FH_1H_2} = \frac{\lambda_{hH_1H_2}}{16\pi^2} \sum_F \left[ g^{LR} m_F C_0 - g^{RR} m_a C_1 - g^{LL} m_b C_2 \right], \quad (D3)$$

$$\Delta_L^{FH} = \frac{g\delta_{hee}}{32\pi^2 m_W (m_a^2 - m_b^2)} \sum_F \left[ m_a m_b m_F g^{RL} (B_0^{(1)} - B_0^{(2)}) + m_F g^{LR} (m_b^2 B_0^{(1)} - m_a^2 B_0^{(2)}) \right. \\ \left. - m_a m_b (g^{RR} m_a + g^{LL} m_b) (B_1^{(1)} - B_1^{(2)}) \right], \quad (D4)$$

$$\Delta_R^{FH} = \frac{g\delta_{hee}}{32\pi^2 m_W (m_a^2 - m_b^2)} \sum_F \left[ m_a m_b m_F g^{LR} (B_0^{(1)} - B_0^{(2)}) + m_F g^{RL} (m_b^2 B_0^{(1)} - m_a^2 B_0^{(2)}) \right. \\ \left. - m_a m_b (g^{LL} m_a + g^{RR} m_b) (B_1^{(1)} - B_1^{(2)}) \right], \quad (D5)$$

where  $g_{ab}^{XY} \equiv g_{aFH_1}^{X*} g_{bFH_2}^Y$  for  $X, Y = L, R$ , and arguments for PV-funtions are  $(m_F^2, m_{H_1}^2, m_{H_2}^2)$ .

The particular formulas of  $\Delta_{L(R)}^{HF_1F_2}$  are

$$\Delta_L^{HFF} = \frac{1}{16\pi^2} \sum_{F_1, F_2} \left\{ g_{hF_{12}}^L \left[ g^{RL} m_{F_1} m_{F_2} C_0 + g^{LR} m_a m_b X_0 \right. \right. \\ \left. \left. + g^{LL} m_a m_{F_2} (C_0 + C_1) + g^{RR} m_b m_{F_1} (C_0 + C_2) \right] \right. \\ \left. + g_{hF_{12}}^R \left[ g^{RL} (B_0^{(12)} + m_H^2 C_0 + m_a^2 C_1 + m_b^2 C_2) \right. \right. \\ \left. \left. + g^{LL} m_a m_{F_1} C_1 + g^{RR} m_b m_{F_2} C_2 \right] \right\}, \quad (D6)$$

$$\Delta_R^{HFF} = \frac{1}{16\pi^2} \sum_{F_1, F_2} \left\{ g_{hF_{12}}^L \left[ g^{LR} (B_0^{(12)} + m_H^2 C_0 + m_a^2 C_1 + m_b^2 C_2) \right. \right. \\ \left. \left. + g^{RR} m_a m_{F_1} C_1 + g^{LL} m_b m_{F_2} C_2 \right] \right. \\ \left. + g_{hF_{12}}^R \left[ g^{LR} m_{F_1} m_{F_2} C_0 + g^{RL} m_a m_b X_0 \right. \right. \\ \left. \left. + g^{RR} m_a m_{F_2} (C_0 + C_1) + g^{LL} m_b m_{F_1} (C_0 + C_2) \right] \right\}, \quad (D7)$$

where  $g^{XY} \equiv g_{aF_1H}^{X*} g_{bF_2H}^Y$  for  $X, Y = L, R$ , and The arguments of PV functions are  $(p_1^2, m_h^2, p_2^2, m_H^2, m_{F_1}^2, m_{F_2}^2)$ .

One-loop contributions from two diagrams 2 and 3 in Fig. 2 containing both Higgs and gauge bosons were introduced previously [101, 112], but they vanish in our numerical investigation because of the suppressed factors  $s_\theta$  and  $s_\delta$ , which are fixed as zeros.

The one-loop contributions given in Eq. (46) are derived by the following transformations:

$$\begin{aligned} \Delta_{L(R)}^{(1)W} &= \Delta_{L(R)}^{nWW} = \sum_{i=1}^{3+2K} \Delta_{L(R)}^{FGG} [F \rightarrow n_i, G \rightarrow W], \\ \Delta_{L(R)}^{(5)W} &= \Delta_{L(R)}^{Wnn} = \sum_{i,j=1}^{3+2K} \Delta_{L(R)}^{GF_1F_2} [F_1 \rightarrow n_i, F_2 \rightarrow n_j, G \rightarrow W], \\ \Delta_{L(R)}^{(7+8)W} &= \Delta_{L(R)}^{nW} = \sum_{i=1}^{3+2K} \Delta_{L(R)}^{FG} [F \rightarrow n_i, G \rightarrow W], \\ \Delta_{L(R)}^{(4)H} &= \sum_{k,l=1}^2 \Delta_{L(R)}^{nH_k^\pm H_l^\pm} = \sum_{k,l=1}^2 \sum_{i=1}^{3+2K} \Delta_{L(R)}^{FH_1H_2} [F \rightarrow n_i, H_1 \rightarrow H_k^\pm, H_2 \rightarrow H_l^\pm], \\ \Delta_{L(R)}^{(6)H} &= \sum_k^2 \Delta_{L(R)}^{H_k^\pm nn} = \sum_k^2 \sum_{i,j=1}^{3+2K} \Delta_{L(R)}^{HF_1F_2} [H \rightarrow H_k^\pm, F_1 \rightarrow n_i, F_2 \rightarrow n_j], \\ \Delta_{L(R)}^{(9+10)H} &= \sum_{k,l=1}^2 \Delta_{L(R)}^{nH_k^\pm} = \sum_{k=1}^2 \sum_{i=1}^{3+2K} \Delta_{L(R)}^{FH} [F \rightarrow n_i, H \rightarrow H_k^\pm]. \end{aligned}$$

- 
- [1] M. Singer, J. W. F. Valle and J. Schechter, Phys. Rev. D **22** (1980), 738
  - [2] V. Pleitez and M. D. Tonasse, Phys. Rev. D **48** (1993), 2353-2355 [arXiv:hep-ph/9301232 [hep-ph]].
  - [3] M. Ozer, Phys. Rev. D **54** (1996), 1143-1149
  - [4] R. Foot, H. N. Long and T. A. Tran, Phys. Rev. D **50** (1994) no.1, R34-R38 [arXiv:hep-ph/9402243 [hep-ph]].
  - [5] R. A. Diaz, R. Martinez and F. Ochoa, Phys. Rev. D **69** (2004), 095009 [arXiv:hep-ph/0309280 [hep-ph]].
  - [6] R. A. Diaz, R. Martinez and F. Ochoa, Phys. Rev. D **72** (2005), 035018 [arXiv:hep-ph/0411263 [hep-ph]].
  - [7] A. J. Buras, F. De Fazio, J. Girrbach and M. V. Carlucci, JHEP **02** (2013), 023 [arXiv:1211.1237 [hep-ph]].

- [8] H. T. Hung, T. T. Hong, H. H. Phuong, H. L. T. Mai and L. T. Hue, Phys. Rev. D **100**, no.7, 075014 (2019) [arXiv:1907.06735 [hep-ph]].
- [9] A. L. Cherchiglia and O. L. G. Peres, JHEP **04** (2023), 017 [arXiv:2209.12063 [hep-ph]].
- [10] A. E. Carcamo Hernandez, R. Martinez and F. Ochoa, Phys. Rev. D **73** (2006), 035007 [arXiv:hep-ph/0510421 [hep-ph]].
- [11] C. Salazar, R. H. Benavides, W. A. Ponce and E. Rojas, JHEP **07** (2015), 096 [arXiv:1503.03519 [hep-ph]].
- [12] L. T. Hue, L. D. Ninh, T. T. Thuc and N. T. T. Dat, Eur. Phys. J. C **78**, no.2, 128 (2018) [arXiv:1708.09723 [hep-ph]].
- [13] E. Suarez, R. H. Benavides, Y. Giraldo, W. A. Ponce and E. Rojas, J. Phys. G **51** (2024) no.3, 035004 [arXiv:2307.15826 [hep-ph]].
- [14] L. T. Hue, K. H. Phan, T. P. Nguyen, H. N. Long and H. T. Hung, Eur. Phys. J. C **82** (2022) no.8, 722 [arXiv:2109.06089 [hep-ph]].
- [15] M. Lindner, M. Platscher and F. S. Queiroz, Phys. Rept. **731** (2018), 1-82 [arXiv:1610.06587 [hep-ph]].
- [16] A. S. De Jesus, S. Kovalenko, F. S. Queiroz, C. Siqueira and K. Sinha, Phys. Rev. D **102**, no.3, 035004 (2020) [arXiv:2004.01200 [hep-ph]].
- [17] Á. S. de Jesus, S. Kovalenko, F. S. Queiroz, C. A. de S. Pires and Y. S. Villamizar, Phys. Lett. B **809** (2020), 135689 [arXiv:2003.06440 [hep-ph]].
- [18] A. Doff and C. A. de S. Pires, Phys. Lett. B **854** (2024), 138733 [arXiv:2403.19338 [hep-ph]].
- [19] I. Chakraborty, H. Roy and T. Srivastava, Nucl. Phys. B **979** (2022), 115780 [arXiv:2106.08232 [hep-ph]].
- [20] I. Chakraborty, H. Roy and T. Srivastava, Eur. Phys. J. C **83** (2023) no.4, 280 [arXiv:2206.07037 [hep-ph]].
- [21] S. Marciano, D. Meloni and M. Parriciatu, JHEP **05** (2024), 020 [arXiv:2402.18547 [hep-ph]].
- [22] J. Gogoi, L. Sarma and M. K. Das, “Leptogenesis and dark matter in minimal inverse seesaw using  $A_4$  modular symmetry,” [arXiv:2311.09883 [hep-ph]].
- [23] D. P. Aguillard *et al.* [Muon g-2], Phys. Rev. Lett. **131** (2023) no.16, 161802 [arXiv:2308.06230 [hep-ex]].
- [24] T. Aoyama, N. Asmussen, M. Benayoun, J. Bijnens, T. Blum, M. Bruno, I. Caprini, C. M. Carloni Calame, M. Cè and G. Colangelo, *et al.* Phys. Rept. **887**, 1-166 (2020)

- [arXiv:2006.04822 [hep-ph]].
- [25] M. Davier, A. Hoecker, B. Malaescu and Z. Zhang, *Eur. Phys. J. C* **71**, 1515 (2011) [erratum: *Eur. Phys. J. C* **72**, 1874 (2012)] [arXiv:1010.4180 [hep-ph]].
- [26] T. Aoyama, M. Hayakawa, T. Kinoshita and M. Nio, *Phys. Rev. Lett.* **109**, 111808 (2012) [arXiv:1205.5370 [hep-ph]].
- [27] T. Aoyama, T. Kinoshita and M. Nio, *Atoms* **7**, no.1, 28 (2019)
- [28] A. Czarnecki, W. J. Marciano and A. Vainshtein, *Phys. Rev. D* **67**, 073006 (2003) [erratum: *Phys. Rev. D* **73**, 119901 (2006)] [arXiv:hep-ph/0212229 [hep-ph]].
- [29] C. Gnendiger, D. Stöckinger and H. Stöckinger-Kim, *Phys. Rev. D* **88**, 053005 (2013) [arXiv:1306.5546 [hep-ph]].
- [30] I. Danilkin and M. Vanderhaeghen, *Phys. Rev. D* **95**, no.1, 014019 (2017) [arXiv:1611.04646 [hep-ph]].
- [31] M. Davier, A. Hoecker, B. Malaescu and Z. Zhang, *Eur. Phys. J. C* **77**, no.12, 827 (2017) [arXiv:1706.09436 [hep-ph]].
- [32] A. Keshavarzi, D. Nomura and T. Teubner, *Phys. Rev. D* **97**, no.11, 114025 (2018) [arXiv:1802.02995 [hep-ph]].
- [33] G. Colangelo, M. Hoferichter and P. Stoffer, *JHEP* **02**, 006 (2019) [arXiv:1810.00007 [hep-ph]].
- [34] M. Hoferichter, B. L. Hoid and B. Kubis, *JHEP* **08**, 137 (2019) [arXiv:1907.01556 [hep-ph]].
- [35] M. Davier, A. Hoecker, B. Malaescu and Z. Zhang, *Eur. Phys. J. C* **80**, no.3, 241 (2020) [erratum: *Eur. Phys. J. C* **80**, no.5, 410 (2020)] [arXiv:1908.00921 [hep-ph]].
- [36] A. Keshavarzi, D. Nomura and T. Teubner, *Phys. Rev. D* **101**, no.1, 014029 (2020) [arXiv:1911.00367 [hep-ph]].
- [37] A. Kurz, T. Liu, P. Marquard and M. Steinhauser, *Phys. Lett. B* **734**, 144-147 (2014) [arXiv:1403.6400 [hep-ph]].
- [38] K. Melnikov and A. Vainshtein, *Phys. Rev. D* **70**, 113006 (2004) [arXiv:hep-ph/0312226 [hep-ph]].
- [39] P. Masjuan and P. Sanchez-Puertas, *Phys. Rev. D* **95**, no.5, 054026 (2017) [arXiv:1701.05829 [hep-ph]].
- [40] G. Colangelo, M. Hoferichter, M. Procura and P. Stoffer, *JHEP* **04**, 161 (2017) [arXiv:1702.07347 [hep-ph]].

- [41] M. Hoferichter, B. L. Hoid, B. Kubis, S. Leupold and S. P. Schneider, *JHEP* **10**, 141 (2018) [arXiv:1808.04823 [hep-ph]].
- [42] A. Gérardin, H. B. Meyer and A. Nyffeler, *Phys. Rev. D* **100**, no.3, 034520 (2019) [arXiv:1903.09471 [hep-lat]].
- [43] J. Bijnens, N. Hermansson-Truedsson and A. Rodríguez-Sánchez, *Phys. Lett. B* **798**, 134994 (2019) [arXiv:1908.03331 [hep-ph]].
- [44] G. Colangelo, F. Hagelstein, M. Hoferichter, L. Laub and P. Stoffer, *JHEP* **03**, 101 (2020) [arXiv:1910.13432 [hep-ph]].
- [45] T. Blum, N. Christ, M. Hayakawa, T. Izubuchi, L. Jin, C. Jung and C. Lehner, *Phys. Rev. Lett.* **124**, no.13, 132002 (2020) [arXiv:1911.08123 [hep-lat]].
- [46] G. Colangelo, M. Hoferichter, A. Nyffeler, M. Passera and P. Stoffer, *Phys. Lett. B* **735**, 90-91 (2014) [arXiv:1403.7512 [hep-ph]].
- [47] V. Pauk and M. Vanderhaeghen, *Eur. Phys. J. C* **74**, no.8, 3008 (2014) [arXiv:1401.0832 [hep-ph]].
- [48] F. Jegerlehner, *Springer Tracts Mod. Phys.* **274**, pp.1-693 (2017)
- [49] M. Knecht, S. Narison, A. Rabemananjara and D. Rabetiariivony, *Phys. Lett. B* **787**, 111-123 (2018) [arXiv:1808.03848 [hep-ph]].
- [50] G. Eichmann, C. S. Fischer and R. Williams, *Phys. Rev. D* **101**, no.5, 054015 (2020) [arXiv:1910.06795 [hep-ph]].
- [51] P. Roig and P. Sanchez-Puertas, *Phys. Rev. D* **101**, no.7, 074019 (2020) [arXiv:1910.02881 [hep-ph]].
- [52] G. Venanzoni [Muon g-2], *PoS EPS-HEP2023* (2024), 037 [arXiv:2311.08282 [hep-ex]].
- [53] D. Hanneke, S. Fogwell and G. Gabrielse, *Phys. Rev. Lett.* **100** (2008), 120801 [arXiv:0801.1134 [physics.atom-ph]].
- [54] R. H. Parker, C. Yu, W. Zhong, B. Estey and H. Müller, *Science* **360** (2018), 191 [arXiv:1812.04130 [physics.atom-ph]].
- [55] X. Fan, T. G. Myers, B. A. D. Sukra and G. Gabrielse, *Phys. Rev. Lett.* **130** (2023) no.7, 071801 [arXiv:2209.13084 [physics.atom-ph]].
- [56] L. Morel, Z. Yao, P. Cladé and S. Guellati-Khélifa, *Nature* **588** (2020) no.7836, 61-65
- [57] T. Aoyama, M. Hayakawa, T. Kinoshita and M. Nio, *Phys. Rev. Lett.* **109** (2012), 111807 [arXiv:1205.5368 [hep-ph]].

- [58] S. Laporta, Phys. Lett. B **772** (2017), 232-238 [arXiv:1704.06996 [hep-ph]].
- [59] T. Aoyama, T. Kinoshita and M. Nio, Phys. Rev. D **97** (2018) no.3, 036001 [arXiv:1712.06060 [hep-ph]].
- [60] H. Terazawa, Nonlin. Phenom. Complex Syst. **21** (2018) no.3, 268-272
- [61] S. Volkov, Phys. Rev. D **100** (2019) no.9, 096004 [arXiv:1909.08015 [hep-ph]].
- [62] A. Gérardin, Eur. Phys. J. A **57** (2021) no.4, 116 [arXiv:2012.03931 [hep-lat]].
- [63] B. Aubert *et al.* [BaBar], Phys. Rev. Lett. **104** (2010), 021802 [arXiv:0908.2381 [hep-ex]].
- [64] K. Afanaciev *et al.* [MEG II], Eur. Phys. J. C **84** (2024) no.3, 216 [arXiv:2310.12614 [hep-ex]].
- [65] A. M. Baldini *et al.* [MEG], Eur. Phys. J. C **76** (2016) no.8, 434 [arXiv:1605.05081 [hep-ex]].
- [66] A. Abdesselam *et al.* [Belle], JHEP **10** (2021), 19 [arXiv:2103.12994 [hep-ex]].
- [67] A. M. Baldini *et al.* [MEG II], Eur. Phys. J. C **78** (2018) no.5, 380 [arXiv:1801.04688 [physics.ins-det]].
- [68] E. Kou *et al.* [Belle-II], PTEP **2019** (2019) no.12, 123C01 [erratum: PTEP **2020** (2020) no.2, 029201] [arXiv:1808.10567 [hep-ex]].
- [69] A. M. Sirunyan *et al.* [CMS], Phys. Rev. D **104** (2021) no.3, 032013 [arXiv:2105.03007 [hep-ex]].
- [70] [ATLAS], “Search for the decays of the Higgs boson  $H \rightarrow ee$  and  $H \rightarrow e\mu$  in  $pp$  collisions at  $\sqrt{s} = 13$  TeV with the ATLAS detector,” ATLAS-CONF-2019-037
- [71] A. Hayrapetyan *et al.* [CMS], Phys. Rev. D **108** (2023) no.7, 072004 [arXiv:2305.18106 [hep-ex]].
- [72] G. Aad *et al.* [ATLAS], JHEP **07** (2023), 166 [arXiv:2302.05225 [hep-ex]].
- [73] Q. Qin, Q. Li, C. D. Lü, F. S. Yu and S. H. Zhou, Eur. Phys. J. C **78** (2018) no.10, 835 [arXiv:1711.07243 [hep-ph]].
- [74] A. Jueid, J. Kim, S. Lee, J. Song and D. Wang, Phys. Rev. D **108** (2023) no.5, 055024 [arXiv:2305.05386 [hep-ph]].
- [75] R. K. Barman, P. S. B. Dev and A. Thapa, Phys. Rev. D **107** (2023) no.7, 075018 [arXiv:2210.16287 [hep-ph]].
- [76] M. Aoki, S. Kanemura, M. Takeuchi and L. Zamakhsyari, Phys. Rev. D **107** (2023) no.5, 055037 [arXiv:2302.08489 [hep-ph]].
- [77] G. Aad *et al.* [ATLAS], Phys. Rev. Lett. **127** (2022), 271801 [arXiv:2105.12491 [hep-ex]].
- [78] G. Aad *et al.* [ATLAS], Phys. Rev. D **108** (2023), 032015 [arXiv:2204.10783 [hep-ex]].

- [79] M. Dam, SciPost Phys. Proc. **1** (2019), 041 [arXiv:1811.09408 [hep-ex]].
- [80] A. Abada *et al.* [FCC], Eur. Phys. J. C **79** (2019) no.6, 474
- [81] D. Jurčiukonis and L. Lavoura, JHEP **03** (2022), 106 [arXiv:2107.14207 [hep-ph]].
- [82] T. T. Hong, Q. D. Tran, T. P. Nguyen, L. T. Hue and N. H. T. Nha, Eur. Phys. J. C **84** (2024) no.3, 338 [arXiv:2312.11427 [hep-ph]].
- [83] A. Abada, J. Kriewald, E. Pinsard, S. Rosauero-Alcaraz and A. M. Teixeira, Eur. Phys. J. C **83** (2023) no.6, 494 [arXiv:2207.10109 [hep-ph]].
- [84] J. G. Korner, A. Pilaftsis and K. Schilcher, Phys. Lett. B **300** (1993), 381-386 [arXiv:hep-ph/9301290 [hep-ph]].
- [85] V. De Romeri, M. J. Herrero, X. Marcano and F. Scarcella, Phys. Rev. D **95** (2017) no.7, 075028 [arXiv:1607.05257 [hep-ph]].
- [86] A. Abada, J. Kriewald and A. M. Teixeira, Eur. Phys. J. C **81** (2021) no.11, 1016 [arXiv:2107.06313 [hep-ph]].
- [87] G. Hernández-Tomé, J. I. Illana, M. Masip, G. López Castro and P. Roig, Phys. Rev. D **101** (2020) no.7, 075020 [arXiv:1912.13327 [hep-ph]].
- [88] A. Crivellin, Z. Fabisiewicz, W. Materkowska, U. Nierste, S. Pokorski and J. Rosiek, JHEP **06** (2018), 003 [arXiv:1802.06803 [hep-ph]].
- [89] A. Ilakovac, A. Pilaftsis and L. Popov, Phys. Rev. D **87** (2013) no.5, 053014 [arXiv:1212.5939 [hep-ph]].
- [90] M. J. Herrero, X. Marcano, R. Morales and A. Szyrkman, Eur. Phys. J. C **78** (2018) no.10, 815 [arXiv:1807.01698 [hep-ph]].
- [91] L. Calibbi, X. Marcano and J. Roy, Eur. Phys. J. C **81** (2021) no.12, 1054 [arXiv:2107.10273 [hep-ph]].
- [92] L. T. Hue and L. D. Ninh, Eur. Phys. J. C **79**, no.3, 221 (2019) [arXiv:1812.07225 [hep-ph]].
- [93] S. Descotes-Genon, M. Moscati and G. Ricciardi, Phys. Rev. D **98** (2018) no.11, 115030 [arXiv:1711.03101 [hep-ph]].
- [94] M. Aoki, S. Kanemura, K. Tsumura and K. Yagyu, Phys. Rev. D **80** (2009), 015017 [arXiv:0902.4665 [hep-ph]].
- [95] A. J. Buras, F. De Fazio and J. Girrbach-Noe, JHEP **08**, 039 (2014) [arXiv:1405.3850 [hep-ph]].
- [96] H. Okada, N. Okada, Y. Orikasa and K. Yagyu, Phys. Rev. D **94**, no.1, 015002 (2016)

- [arXiv:1604.01948 [hep-ph]].
- [97] H. N. Long, N. V. Hop, L. T. Hue and N. T. T. Van, Nucl. Phys. B **943** (2019), 114629 [arXiv:1812.08669 [hep-ph]].
- [98] A. S. de Jesus, S. Kovalenko, T. B. de Melo, J. P. Neto, Y. M. Oviedo-Torres, F. S. Queiroz, Y. S. Villamizar and A. R. Zerwekh, Phys. Lett. B **849** (2024), 138419 [arXiv:2304.00041 [hep-ph]].
- [99] A. Alves, L. Duarte, S. Kovalenko, Y. M. Oviedo-Torres, F. S. Queiroz and Y. S. Villamizar, Phys. Rev. D **106** (2022) no.5, 055027 [arXiv:2203.02520 [hep-ph]].
- [100] A. E. Cárcamo Hernández, L. Duarte, A. S. de Jesus, S. Kovalenko, F. S. Queiroz, C. Siqueira, Y. M. Oviedo-Torres and Y. Villamizar, Phys. Rev. D **107** (2023) no.6, 063005 [arXiv:2208.08462 [hep-ph]].
- [101] T. T. Hong, N. H. T. Nha, T. P. Nguyen, L. T. T. Phuong and L. T. Hue, PTEP **2022** (2022), 9 [arXiv:2206.08028 [hep-ph]].
- [102] L. T. Hue, H. T. Hung, N. T. Tham, H. N. Long and T. P. Nguyen, Phys. Rev. D **104** (2021) no.3, 033007 [arXiv:2104.01840 [hep-ph]].
- [103] A. Ibarra, E. Molinaro and S. T. Petcov, JHEP **09** (2010), 108 [arXiv:1007.2378 [hep-ph]].
- [104] E. Arganda, M. J. Herrero, X. Marcano and C. Weiland, Phys. Rev. D **91** (2015) no.1, 015001 [arXiv:1405.4300 [hep-ph]].
- [105] J. A. Casas and A. Ibarra, Nucl. Phys. B **618** (2001), 171-204 [arXiv:hep-ph/0103065 [hep-ph]].
- [106] L. T. Hue, A. E. Cárcamo Hernández, H. N. Long and T. T. Hong, Nucl. Phys. B **984** (2022), 115962 [arXiv:2110.01356 [hep-ph]].
- [107] A. Crivellin, M. Hoferichter and P. Schmidt-Wellenburg, Phys. Rev. D **98** (2018) no.11, 113002 [arXiv:1807.11484 [hep-ph]].
- [108] L. Lavoura, Eur. Phys. J. C **29** (2003), 191-195 [arXiv:hep-ph/0302221 [hep-ph]].
- [109] H. K. Dreiner, H. E. Haber and S. P. Martin, Phys. Rept. **494** (2010), 1-196 [arXiv:0812.1594 [hep-ph]].
- [110] E. Arganda, A. M. Curiel, M. J. Herrero and D. Temes, Phys. Rev. D **71** (2005), 035011 [arXiv:hep-ph/0407302 [hep-ph]].
- [111] T. P. Nguyen, T. T. Le, T. T. Hong and L. T. Hue, Phys. Rev. D **97** (2018) no.7, 073003 [arXiv:1802.00429 [hep-ph]].

- [112] L. T. Hue, H. N. Long, T. T. Thuc and T. Phong Nguyen, Nucl. Phys. B **907** (2016), 37-76 [arXiv:1512.03266 [hep-ph]].
- [113] A. Denner, S. Heinemeyer, I. Puljak, D. Rebuszi and M. Spira, Eur. Phys. J. C **71** (2011), 1753 [arXiv:1107.5909 [hep-ph]].
- [114] R. L. Workman [Particle Data Group], PTEP **2022**, 083C01 (2022)
- [115] N. Aghanim *et al.* [Planck], Astron. Astrophys. **641** (2020), A6 [erratum: Astron. Astrophys. **652** (2021), C4] [arXiv:1807.06209 [astro-ph.CO]].
- [116] E. Fernandez-Martinez, J. Hernandez-Garcia and J. Lopez-Pavon, JHEP **08** (2016), 033 [arXiv:1605.08774 [hep-ph]].
- [117] N. R. Agostinho, G. C. Branco, P. M. F. Pereira, M. N. Rebelo and J. I. Silva-Marcos, Eur. Phys. J. C **78** (2018) no.11, 895 [arXiv:1711.06229 [hep-ph]].
- [118] M. Blennow, E. Fernández-Martínez, J. Hernández-García, J. López-Pavón, X. Marcano and D. Naredo-Tuero, JHEP **08** (2023), 030 [arXiv:2306.01040 [hep-ph]].
- [119] P. Escribano, J. Terol-Calvo and A. Vicente, Phys. Rev. D **103**, no.11, 115018 (2021) [arXiv:2104.03705 [hep-ph]].
- [120] C. Biggio, E. Fernandez-Martinez, M. Filaci, J. Hernandez-Garcia and J. Lopez-Pavon, JHEP **05** (2020), 022 [arXiv:1911.11790 [hep-ph]].
- [121] J. P. Pinheiro, C. A. de S. Pires, F. S. Queiroz and Y. S. Villamizar, Phys. Lett. B **823** (2021), 136764 [arXiv:2107.01315 [hep-ph]].
- [122] B. L. Sánchez-Vega, G. Gambini and C. E. Alvarez-Salazar, Eur. Phys. J. C **79**, no.4, 299 (2019) [arXiv:1811.00585 [hep-ph]].
- [123] F. J. Botella, F. Cornet-Gomez, C. Miró and M. Nebot, Eur. Phys. J. C **82** (2022), 915 [arXiv:2205.01115 [hep-ph]].
- [124] A. Das and N. Okada, Phys. Rev. D **88** (2013), 113001 [arXiv:1207.3734 [hep-ph]].
- [125] A. Das and N. Okada, Phys. Lett. B **774** (2017), 32-40 [arXiv:1702.04668 [hep-ph]].
- [126] A. Das, Int. J. Mod. Phys. A **36** (2021) no.04, 2150012 [arXiv:1701.04946 [hep-ph]].
- [127] A. Bhardwaj, A. Das, P. Konar and A. Thalapillil, J. Phys. G **47** (2020) no.7, 075002 [arXiv:1801.00797 [hep-ph]].
- [128] A. Costantini, M. Ghezzi and G. M. Pruna, Phys. Lett. B **808** (2020), 135638 [arXiv:2001.08550 [hep-ph]].
- [129] T. Li, J. Pei and W. Zhang, Eur. Phys. J. C **81** (2021) no.7, 671 [arXiv:2104.03334 [hep-ph]].

- [130] C. H. Chen, C. W. Chiang and C. W. Su, J. Phys. G **51** (2024) no.8, 085001 [arXiv:2301.07070 [hep-ph]].
- [131] S. Iguro, T. Kitahara, M. S. Lang and M. Takeuchi, Phys. Rev. D **108** (2023) no.11, 11 [arXiv:2304.09887 [hep-ph]].
- [132] S. Ghosh and P. Ko, “Explaining ATOMKI,  $(g - 2)_\mu$ , and MiniBooNE anomalies with light mediators in  $U(1)_H$  extended model,” [arXiv:2311.14099 [hep-ph]].
- [133] E. Arganda, M. J. Herrero, X. Marcano, R. Morales and A. Szyrkman, Phys. Rev. D **95** (2017) no.9, 095029 [arXiv:1612.09290 [hep-ph]].
- [134] N. H. Thao, L. T. Hue, H. T. Hung and N. T. Xuan, Nucl. Phys. B **921** (2017), 159-180 [arXiv:1703.00896 [hep-ph]].
- [135] G. Hernández-Tomé, J. I. Illana and M. Masip, Phys. Rev. D **102** (2020) no.11, 113006 [arXiv:2005.11234 [hep-ph]].
- [136] R. S. Hundi, Eur. Phys. J. C **82** (2022) no.6, 505 [arXiv:2201.03779 [hep-ph]].
- [137] Z. Fan and K. Yagyu, JHEP **06** (2022), 014 [arXiv:2201.11277 [hep-ph]].
- [138] P. Athron, C. Balázs, D. H. J. Jacob, W. Kotlarski, D. Stöckinger and H. Stöckinger-Kim, JHEP **09** (2021), 080 [arXiv:2104.03691 [hep-ph]].
- [139] S. Li, Z. Li, F. Wang and J. M. Yang, Nucl. Phys. B **983** (2022), 115927 [arXiv:2205.15153 [hep-ph]].
- [140] E. Arganda, M. J. Herrero, X. Marcano and C. Weiland, Phys. Rev. D **93** (2016) no.5, 055010 [arXiv:1508.04623 [hep-ph]].
- [141] Z. N. Zhang, H. B. Zhang, J. L. Yang, S. M. Zhao and T. F. Feng, Phys. Rev. D **103** (2021) no.11, 115015 [arXiv:2105.09799 [hep-ph]].
- [142] M. Zeleny-Mora, J. L. Díaz-Cruz and O. Félix-Beltrán, Int. J. Mod. Phys. A **37** (2022) no.36, 2250226 [arXiv:2112.08412 [hep-ph]].
- [143] X. Marcano and R. A. Morales, Front. in Phys. **7** (2020), 228 [arXiv:1909.05888 [hep-ph]].
- [144] A. Brignole and A. Rossi, Phys. Lett. B **566** (2003), 217-225 [arXiv:hep-ph/0304081 [hep-ph]].
- [145] P. T. Giang, L. T. Hue, D. T. Huong and H. N. Long, Nucl. Phys. B **864** (2012), 85-112 [arXiv:1204.2902 [hep-ph]].
- [146] E. Arganda, M. J. Herrero, R. Morales and A. Szyrkman, JHEP **03** (2016), 055 [arXiv:1510.04685 [hep-ph]].

- [147] M. A. Arroyo-Ureña, J. L. Díaz-Cruz, O. Félix-Beltrán and M. Zeleny-Mora, [arXiv:2308.01380 [hep-ph]].
- [148] K. Huitu and N. Koivunen, JHEP **10**, 065 (2019) [arXiv:1905.05278 [hep-ph]].
- [149] G. 't Hooft and M. J. G. Veltman, Nucl. Phys. B **44** (1972), 189-213
- [150] A. Denner and S. Dittmaier, Nucl. Phys. B **734** (2006), 62-115 [arXiv:hep-ph/0509141].
- [151] T. P. Nguyen, T. T. Thuc, D. T. Si, T. T. Hong and L. T. Hue, PTEP **2022** (2022) no.2, 023B01 [arXiv:2011.12181 [hep-ph]].
- [152] T. Hahn and M. Perez-Victoria, Comput. Phys. Commun. **118** (1999), 153-165 [arXiv:hep-ph/9807565 [hep-ph]].
- [153] S. Centelles Chuliá, R. Srivastava and A. Vicente, JHEP **03** (2021), 248 [arXiv:2011.06609 [hep-ph]].
- [154] R. Calabrese, A. O. M. Iorio, S. Morisi, G. Ricciardi and N. Vignaroli, Phys. Rev. D **109** (2024) no.5, 055030 [arXiv:2312.02287 [hep-ph]].
- [155] R. Calabrese, A. De Iorio, D. F. G. Fiorillo, A. O. M. Iorio, S. Morisi and G. Miele, Phys. Rev. D **104** (2021) no.5, 055006 [arXiv:2104.06720 [hep-ph]].
- [156] J. E. Cieza Montalvo, N. V. Cortez, J. Sa Borges and M. D. Tonasse, Nucl. Phys. B **756** (2006), 1-15 [erratum: Nucl. Phys. B **796** (2008), 422-423] [arXiv:hep-ph/0606243 [hep-ph]].
- [157] S. Chatrchyan *et al.* [CMS], JHEP **07** (2013), 122 [erratum: JHEP **11** (2022), 149] [arXiv:1305.0491 [hep-ex]].
- [158] L. Hue and L. Ninh, Mod. Phys. Lett. A **31** (2016) no.10, 1650062 [arXiv:1510.00302 [hep-ph]].
- [159] V. Pleitez, “Challenges for the 3-3-1 models,” [arXiv:2112.10888 [hep-ph]].
- [160] E. R. Barreto and A. G. Dias, “Fractionary Charged Particles Confronting Lepton Flavor Violation and the Muon’s Anomalous Magnetic Moment,” [arXiv:2307.01382 [hep-ph]].
- [161] [CMS], in proton-proton collisions at  $\sqrt{s} = 13$  TeV,” CMS-PAS-EXO-18-002.
- [162] G. Aad *et al.* [ATLAS], Phys. Lett. B **847** (2023), 138316 [arXiv:2303.13613 [hep-ex]].
- [163] A. M. Sirunyan *et al.* [CMS], JHEP **07** (2019), 142 [arXiv:1903.04560 [hep-ex]].
- [164] G. Aad *et al.* [ATLAS], JHEP **06** (2021), 145 [arXiv:2102.10076 [hep-ex]].
- [165] N. Haba and K. Tsumura, JHEP **06** (2011), 068 [arXiv:1105.1409 [hep-ph]].
- [166] C. Guo, S. Y. Guo, Z. L. Han, B. Li and Y. Liao, JHEP **04** (2017), 065 [arXiv:1701.02463 [hep-ph]].

[167] Y. L. Tang, Phys. Rev. D **98** (2018) no.3, 035043 [arXiv:1712.10108 [hep-ph]].